

Chick chorioallantoic membrane: a valuable 3D *in vivo* model for screening nanoformulations for tumor antiangiogenic therapeutics

ANNA SENRUNG^{1,2}, TANYA TRIPATHI¹, DIVYA JANJUA¹, SUNITA KUMARI YADAV², ARUN CHHOKAR^{1,3}, NIKITA AGGARWAL¹, JONI YADAV¹, APOORVA CHAUDHARY¹, UDIT JOSHI¹, PALLAVI SETHI², ALOK CHANDRA BHARTI^{*1}

¹Molecular Oncology Laboratory, Department of Zoology, University of Delhi (North Campus), Delhi, India,

²Neuropharmacology and Drug Delivery Laboratory, Daulat Ram College, University of Delhi, Delhi, India,

³Department of Zoology, Deshbandhu College, University of Delhi, Delhi, India

ABSTRACT Drug discovery is an extensive process. From identifying lead compounds to approval for clinical application, it goes through a sequence of labor-intensive *in vitro*, *in vivo* preclinical screening and clinical trials. Among thousands of drugs screened only a few get approval for clinical trials. Furthermore, these approved drugs are often discontinued due to systemic toxicity and comorbidity at clinically administered dosages. To overcome these limitations, nanoformulations have emerged as the most sought-after strategy to safely and effectively deliver drugs within tumors at therapeutic concentrations. Most importantly, the employment of suitably variable preclinical models is considered highly critical for the therapeutic evaluation of candidate drugs or their formulations. A review of literature from the past 10 years on antiangiogenic nanoformulations shows the employment of limited types of preclinical models mainly the 2-dimensional (2D) monolayer cell culture and murine models as the mainstay for drug uptake, toxicity and efficiency studies. To top it all, murine models are highly expensive, time-consuming and require expertise in handling them. The current review highlights the utilization of the age-old chicken chorioallantoic membrane (CAM), a well-defined angiogenic model in the investigation of antiangiogenic compounds and nanoformulations in an economic framework. For practical applicability, we have evaluated the CAM model to demonstrate the screening of antiangiogenic compounds and that tumor cells can be implanted onto developing CAM for growing xenografts by recruiting host endothelial and other cellular components. In addition, the exploitation of CAM tumor xenograft models for the evaluation of nanoparticle distribution has also been reinforced by demonstrating that intravenously administered iron oxide nanoparticles (IONPs) passively accumulate and exhibit intracellular as well as extracellular compartment accumulation in highly vascular xenografts. Finally, the ethical considerations, benefits, and drawbacks, of using CAM as an experimental model for testing potential therapeutics are also highlighted.

KEYWORDS: chorioallantoic membrane, antiangiogenesis, tumor xenograft, nanoparticles, chick *in vivo* model, candidate drug screening

1. Introduction

Patients diagnosed with tumor undergo surgery, radio- and/or chemotherapy depending on the type and stage of the tumor. The growing arsenal of oncology tools is elaborate, however, many technical impediments, such as the genetic instability of tumor cells, the inter- and intra-heterogenic nature of tumors, and the development of resistance or evasion of drugs by tumor cells prevent desired impact of these drugs. Failure to deliver a drug in optimal dose, as well as lack of efficient targeted delivery mechanism, often leads

to severe systemic toxicity and treatment-associated morbidity. The pursuit of drugs that are safe and effectively delivered to the target site is the key research area. Angiogenesis, the formation of new blood vessels from pre-existing blood vessels, is the key driver

Abbreviations used in this paper: CAM, chorioallantoic membrane; DOX, doxorubicin; EDD, embryonic development day; GS, gelatin sponge; HH, Hamburger and Hamilton stages; H&E, hematoxylin & eosin; IHC, immunohistochemistry; IONP, iron oxide nanoparticle; IRT, irinotecan; NC, nanocarrier; NP, nanoparticle; RH, relative humidity; TME, tumor microenvironment.

*Address correspondence to: Alok Chandra Bharti. Molecular Oncology Laboratory, Department of Zoology, University of Delhi, Delhi - 110007, India.
E-mail: alokchandrab@yahoo.com | https://orcid.org/0000-0002-5996-2832

of tumor sustenance, proliferation, growth, migration or metastasis and has emerged as the primary target for anti-tumor therapies. However, the pre-clinical models for testing the anti-angiogenic potential of new drugs are limited.

An explicitly effective chemotherapeutic potential of a drug can only be appraised with the help of efficient *in vitro* and *in vivo* preclinical model systems candidate (Alphandéry, 2018). By convention, *in vitro*, preclinical screening of potential drugs is followed by *in vivo* preclinical studies. For *in vivo* preclinical models, immunocompromised mice are most commonly employed for developing orthotopic tumors as well as facilitating the screening of potential chemotherapeutic drugs and their nanocarriers (NCs). Although murine models are optimal for mimicking different forms of cancer reported in clinics, research involving transgenic mice is expensive as well as time-consuming. On average, implantation of tumor xenograft can only be performed after 4 weeks of birth. Monitoring and evaluation of tumor growth have to be performed for 4-6 weeks with ethical clearance from the institutional animal ethical committee (Kunz et al., 2019). Efficacy studies are often jeopardized by ulcerations in developing tumors, signs of pain or sudden demise of the mouse. This powerful technique is associated with the suffering of animals as well as requires an elaborate infrastructure. Considering monetary aspects, ethical issues and expertise requirement, it becomes furthermore important to look for an alternative/supplementary preclinical *in vivo* model system for the evaluation of drugs or NCs before moving on to higher models. This will help reduce the usage of murine models as well as increase the credibility of the test

drug for clinical application being evaluated in multiple systemic models. Several simple model systems like zebrafish, *Drosophila*, and chick chorioallantoic membrane (CAM) models are potential alternatives for oncology studies. Amongst these models, the chick being homeothermic, the chick CAM bears the closest physiological relevance for the evaluation of pharmacokinetics and -dynamics of drugs for human application.

In the current manuscript, the suitability of CAM standalone and CAM tumor xenograft models exploited to screen antiangiogenic compounds, and their exploitation for the evaluation of nanoformulations as antiangiogenic therapeutics is highlighted. The study emphasizes the benefits of using CAM as an alternative or supplementary *in vivo* cancer model. Furthermore, the review has been supported by model experimental study carried out in our laboratory to enable researchers with no prior experience in the practical applicability of the CAM model.

2. Chick CAM model

Chick CAM is an extraembryonic membrane, a very thin layer (rarely exceeding 100 μm thickness) formed by the fusion of the mesodermal layer of the outer wall of allantois with the adjoining mesodermal layer of the chorion (Deryugina and Quigley, 2008; Melkonian et al., 2002). Histologically, CAM comprises mainly, 1) the ectoderm adjacent to the shell membrane, 2) the mesoderm rich in blood vessels and other stromal components, and 3) the endoderm adjacent to the allantoic cavity (Deryugina and Quigley,

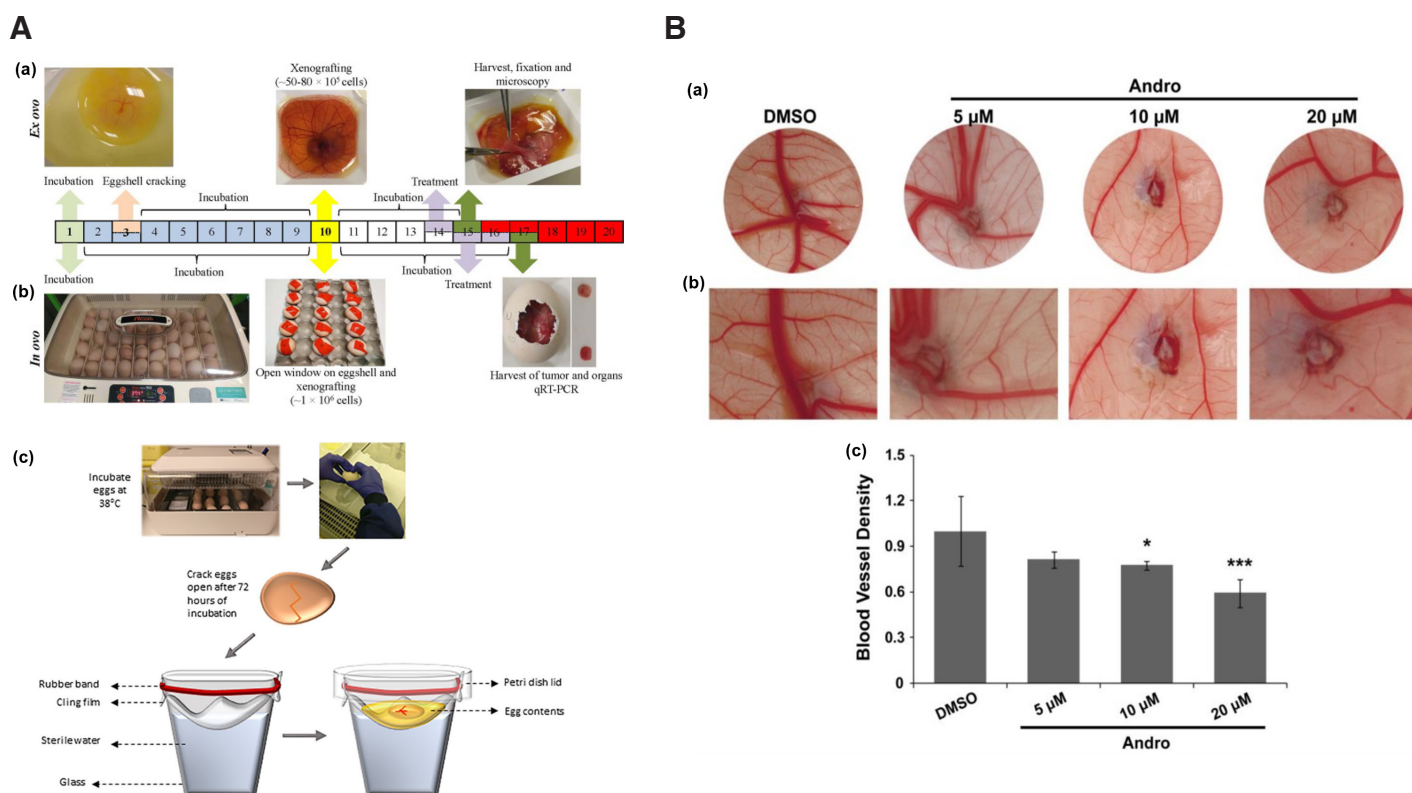


Fig. 1. Chick embryo culture as an experimental model. (A) (a) *Ex ovo* boat culture method, (b) *in ovo* window culture method adapted from (Merlos Rodrigo et al., 2021) and (c) *ex ovo* hammock culture method. Adapted from (Kohli et al., 2020). (B) (a) Images showing antiangiogenic activity of andrographolide (Andro) at different concentrations, (b) at higher magnification and (c) graphical representation of the antiangiogenic activity of andrographolide. Adapted from (Dai et al., 2017). All images are licensed under CC BY.

TABLE 1

CHICK EMBRYO SURVIVABILITY USING DIFFERENT CULTURE METHODS AND THEIR APPLICABILITY AS ANGIOGENESIS MODEL

Method	Time frame	Temperature	Humidity	% Survival	Reference	Advantages	Disadvantages
Windowing	Up to EDD13	37°C	50%	85–95%	(Naik <i>et al.</i> , 2018)	<ul style="list-style-type: none"> • Cost-effective. • Wider range of tolerance to physical factors. • Suitable for tumor xenograft angiogenesis assay. 	<ul style="list-style-type: none"> • Limited access to CAM. Surface area for experimental manipulation. • Not suitable for direct chick CAM angiogenesis assay. • Difficulty in imaging with good resolution.
	Up to EDD18	37.8 °C	70%	>80%	(Kunz <i>et al.</i> , 2019)		
	Up to EDD14	37°C	60%	70%	(Lokman <i>et al.</i> , 2012)		
	At EDD7	37.5 °C	N/A	67.96%	(Eckrich <i>et al.</i> , 2020)		
	Up to EDD8.5	38°C	60%	63%	(Andacht <i>et al.</i> , 2004)		
	Up to EDD8	38 °C	75%	50%	(Ridderbusch <i>et al.</i> , 2015)		
Boat	Up to EDD11	37.5°C	60%	45.2-75%	(Borwompinyo <i>et al.</i> , 2005)	<ul style="list-style-type: none"> • Larger CAM surface area for experimental manipulation. • Suitable for both direct CAM and tumor xenograft angiogenesis assays. • Easy visualization and imaging with good resolution. 	<ul style="list-style-type: none"> • Narrow range of tolerance to physical factors. • Slightly expensive than windowing method.
	Up to EDD14	37- 38° C	60%	>80%	(Mangir <i>et al.</i> , 2019)		
	Up to EDD13	37°C	50%	15–25%	(Naik <i>et al.</i> , 2018)		
	Up to EDD14	37°C	60%	10%	(Lokman <i>et al.</i> , 2012)		
Hammock	Up to EDD13	37°C	50%	85–95%	(Naik <i>et al.</i> , 2018)	<ul style="list-style-type: none"> • Cost-effective. • Moderate CAM surface area for experimental manipulation (intermediate to windowing and Boat method). • Suitable for both direct CAM and tumor xenograft angiogenesis assays. 	<ul style="list-style-type: none"> • Narrow range of tolerance to physical factors. • Extra caution requirement in handling. • Slightly expensive than windowing method.
	Up to EDD14	38°C	80%-90%	60%	(Kohli <i>et al.</i> , 2020)		
	Up to EDD8	37°C	60%	50%	(Dugan <i>et al.</i> , 1991)		
	Up to EDD14	38 °C	80%	Up to 17%	(Tahara <i>et al.</i> , 2021)		

[i] Abbreviations: EDD, Embryonic development day.

2008). CAM being an embryonic tissue and naturally perfused with blood vessels makes it an ideal model for studies associated with blood vessels including tumor angiogenesis or intravenous drug delivery evaluation. CAM additionally is attributed with several features pragmatic for application as a cancer biomedical model. Chick CAM up to embryonic development day (EDD) 14 lacks innervation and is considered to impart no pain to the developing embryo (Eckrich *et al.*, 2020; Schmitd *et al.*, 2019) meeting the 3R strategies by Russel and Burch (Hubrecht and Carter, 2019). Usage of CAM for experimentation up to day 14 of embryonic development generally does not require any ethical clearance (Dhara *et al.*, 2018; Robl *et al.*, 1991). Interestingly, experimental manipulations on tumor angiogenesis or antiangiogenic drugs and nanoformulation screening with CAM models can be performed and completed before the embryo grows beyond day 14 of its developmental period, i.e., the first two-thirds of its incubation period (considering the total incubation period to be 21 days). Despite these virtues, the number of articles published in the last 10 years according to PubMed search using the keywords ‘chick CAM nanoparticles’, ‘murine nanoparticles’, ‘chick CAM angiogenesis and ‘murine angiogenesis’ resulted in 92, 39516, 586, and 22729 articles, respectively (accessed August 2023). These trends indicate a disproportionately low-frequency use of this valuable age-old model system (CAM model) for new applications. Clearly, there is a need for greater recognition of the benefits of CAM model usage.

To employ chick culture for cancer angiogenesis experimentation, the working area needs to be increased for manipulation and implantation of tumors on the vascular bed of CAM. Several studies have extensively described simple as well as economical procedure for opening and shell-less culturing of chick embryos within the laboratory. Several choices of *ex ovo* and *in ovo* chick embryo culture methods/conditions are available such as: petri dish (Auerbach *et al.*, 1974; Dohle *et al.*, 2009), polystyrene plastic wrap, polymethylpentene film, polyurethane membranes suspended from plastic tripod/cup (Buskohl, 2012; Dugan *et al.*, 1991; Dunn and Boone, 1978; Dunn *et al.*, 1981; Kamihiro *et al.*, 1998; Scott *et al.*, 1993; Tahara and Obara, 2014; Yalcin *et al.*, 2010a), plastic weigh boats (Dorrell *et al.*, 2012; Scott *et al.*, 1993), plastic cups with rounded bottoms (Jakobson

et al., 1989), and eggshell windowing (Farzaneh *et al.*, 2018). The ‘*ex ovo*’ expression is used in the technique of culturing chick embryos for boat/hammock method, which involves incubating them outside the eggshell in an artificial environment, facilitating easier access and manipulation of the developing embryo for experimental purposes. On the other hand, the *in ovo* windowing method maintains the chick embryos within their natural environment, inside the eggshell. Since CAM development and assays performed on this tissue are performed in live embryonic conditions, *in vivo* expression is exclusively used by many investigators to refer to manipulation of CAM tissue in fertilized live embryos. Amongst the several methods available, three methods i.e., windowing (*in ovo*), boat (*ex ovo*), and hammock (*ex ovo*) type are the most commonly employed methods in therapeutic screening study. Window method involves culturing the chick embryo in its normal setup, where a small cut/window is made through the eggshell for visualization and experimental manipulation (Fig. 1A middle panel). The area of the cut could vary on the need of the experiment. The latter two are shell-less culture (*ex ovo*) techniques where the whole content of the fertilized egg is poured into a culture vessel. In the case of the boat method, the chick embryo development is generally maintained in a weigh boat (Fig. 1A top panel). The Hammock method involves suspending a membrane from a transparent/plastic tripod/cup (Fig. 1A bottom panel). The suspended membrane is generally oval-shaped to closely recapitulate the normal egg shape. Into the oval-shaped membrane, the whole content of the fertilized egg is emptied and maintained for experimental manipulation. The optimal model is generally determined based on survival, working area for experimental manipulation, area of respiratory gaseous exchange and ease of transportation. The chick embryo survivability using different culture methods under various temperature and humidity conditions along with their applicability as an angiogenesis model is given in Table 1. Barring a few reports, the survivability of chick embryos in the window method is far superior to boat or hammock methods. However, it gives relatively lesser area for experimental manipulation. In terms of the cost, the window method is highly cost effective and economical in comparison to boat and hammock. However, it might differ based on the materials used.

3. Application of CAM in oncology

3.1. CAM standalone as in vivo angiogenesis model

Tumor endothelial cells (ECs) often exhibit differential responses from normal blood vasculature, however, chick embryonic developmental ECs and tumor angiogenesis utilize a similar network of growth factors, receptors and signaling pathways (Ziyad and Iruela-Arispe, 2011). In other words, developmental vasculogenesis (blood vessel formation *de novo*) and tumor angiogenesis (development of blood vessels from pre-existing blood vessels) processes have common molecular signals, such as vascular endothelial growth factor (VEGF), fibroblast growth factor 2 (FGF2), platelet-derived growth factor (PDGF), transforming growth factor beta (TGFB1), angiopoietin 1/2 among others (Goldie et al., 2008; Kubis and Levy, 2003; Lugano et al., 2020; Vargesson, 2003). This interesting phenomenon and the intense angiogenic nature of the chick CAM makes it a very reliable and attractive tumor angiogenic model (Fig. 1B). By EDD8, the CAM blood vessels comprise of small arterioles and venules lying within the mesoderm and extensive capillary network located beneath the chorionic ectoderm (Ausprunk et al., 1974). Progressive changes have been observed in CAM blood vessel ECs from EDD8 to EDD18 with significant growth

and remodeling up to EDD14 making it highly responsive to both pro- and anti-angiogenic stimuli (Ausprunk et al., 1974; Dupont et al., 2002). Many researchers working on tumor angiogenesis using CAM standalone model (CAM without tumor cell implantation), optimized their studies around EDD8-14/15. The finding of the antiangiogenic role of exosomes derived from stem cells of human deciduous exfoliated teeth using CAM was evaluated from EDD8 to EDD10 (Liu et al., 2022). The pro-angiogenic property of sodium arsenite and reversal activity by various selenium-derived compounds (dimethyl selenone, diphenyl selenone, sodium selenite or Se-methyl selenocysteine) was determined on CAM between EDD10-14 (Mousa et al., 2007). Using CAM of 12–15 day old chick embryo, intense pro-angiogenic activity of a novel sulfonamide-chalcone hybrid was studied (Silva et al., 2022). Literature suggests that anti-angiogenic effects on chick CAM can be determined by measuring blood vessel density, diameter, thickness, length, branch points, total area of CAM (Ribatti, 2016), disorganization, bending or looping of vessels (Tufan and Satiroglu-Tufan, 2005) at or around the site of test compound application. Using CAM standalone angiogenesis assay, several natural and synthetic compounds have been evaluated for their antiangiogenic activity. It has been conveniently utilized for screening compounds of

TABLE 2

REPRESENTATIVE STUDIES SHOWING CHICK CAM AS STANDALONE MODEL FOR SCREENING OF POTENTIAL ANTIANGIOGENIC COMPOUNDS

Antiangiogenic compounds	Nature of compounds	Treatment/active concentration	Time frame	Effects on CAM angiogenesis	Method	Reference
B-9-3	Derivative of harmine	0.31, 2.5 & 20 µg/egg	EDD7-EDD10	↓ number of blood vessels & branch points	Window	(Ma et al., 2016)
D-limonene	Monocyclic monoterpene	1, 5 & 10 µg loaded on 1 mm ² GS (pre-soaked)	EDD8-EDD12	↓ number of blood vessels dose-dependently	Window	(Shah et al., 2018)
Docosahexaenoic acid (DHA)	Omega-3 fatty acid	1, 10, 100 µM & 1 mM loaded on filter paper disc	EDD7-EDD9	↓ number of vessels in a dose-dependent manner.	Window	(Pal et al., 2019)
Epigallocatechin gallate	A phenolic antioxidant	250 µg/ml (100 µl) loaded on 5mm diameter filter disc	EDD7-EDD10	↓ inhibited blood vessels with diameters ≤0.2 mm	Window	(Liao et al., 2020)
Galangin	Natural flavonoid	20 µM loaded on filter disc	EDD5-EDD7	Disrupted angiogenesis with attenuated microvessels & fewer angiogenic vessels	Window	(Chen et al., 2019)
(±)-Gossypol	Natural polyphenolic	15, 30, 60 & 120 mM loaded 0.5 cm diameter filter paper	EDD7-EDD8	Dose-dependent anti-angiogenic effects	Window	(Ulus et al., 2018)
Luteolin	Tetrahydroxyflavone	1 nM, 1 µM & 1 mM	EDD11-EDD12/13	↓ angiogenesis	Window	(Ambasta et al., 2015)
Miet	Ethanol extract of <i>Melilotus indicus</i>	200 µg/ml on filter paper disc	EDD6/7-EDD7/8	↓ BV formation.	Window	(Saleem et al., 2021)
Myricetin	Hexahydroxyflavone	25, 50 & 100 µmol (20 µl) in DMSO	EDD9-EDD11	↓ density of the vascular plexus	Window	(Zhou et al., 2019)
Naringenin	Abietane diterpenoid	25 & 50 nmol/egg on glass coverslips (1 mm ²)	EDD8-EDD10	↓ BV numbers & branching patterns.	Window	(Li et al., 2016)
Polyisoprenylated cysteinyl amide inhibitor: NSL-BA-040	Synthetic	0.12, 0.30 & 0.60 µg in 50 µl DPBS	EDD8-EDD10	↓ number of vessels & branches in a concentration-dependent manner; virtually no vessels at 0.60 µg.	Window	(Nkembo et al., 2016)
Ruthenium(II)-p-cymene complex 2	Organometallic	42 µM, 0.47 mg/kg (80 µl) in DMSO + 0.9% NaCl daily from EDD11-EDD14	EDD11,12,13,14-EDD15	Presence of avascular zones; ↓ branching point.	Window	(Nowak-Sliwinska et al., 2015)
Scutellarin	Glycosyloxyflavone	0.5, 1 & 2 µM suspended on sterile filter paper	EDD8-EDD13	↓ micro-vessel formation	Window	(Zhu et al., 2017)
Shikonin	Naphthoquinone	0.025, 0.05 & 0.1 pM place within silicone ring (12 mm × 10 mm × 1 mm diameter)	EDD6-EDD8	Distorted vascular architecture; ↓ number of BV (inhibition of new blood vessel formation)	Window	(Liu et al., 2020)
Tanshinone I	Abietane diterpenoid	0.01, 0.1, 1, 10 & 100 µM dried on coverslips	EDD7-EDD9	Attenuated neovascularization	Window	(Wang et al., 2015b)
Tanshinone IIA	Lipophilic active constituent of <i>Salvia miltiorrhiza</i> root	2.5, 5, 10 & 20 µM dried on coverslips	EDD7-EDD9	↓ BV formation	Window	(Sui et al., 2017)
Thalidomide derivatives (8 compounds)	Synthetic analogs of thalidomide	5 mg/ml (20 µl) on filter paper disc (2 mm diameter)	EDD10-EDD12	Two compounds (2a & 2b) showed ↓ of vessels' number, neovascularization area & total length of vessels.	Window	(da Costa et al., 2015)

[i] Abbreviations: BV-Blood vessel, CA-4-Combretastatin A-4, CM-conditioned media, DPBS-Dulbecco's Phosphate-Buffered Saline, GS-Gelatin sponge, HBSS-Hank's balanced salt solution, YF-452-N-(N-pyrrolidylacetyl)-9-(4-bromobenzyl)-1,3,4,9-tetrahydro-β-carboli.

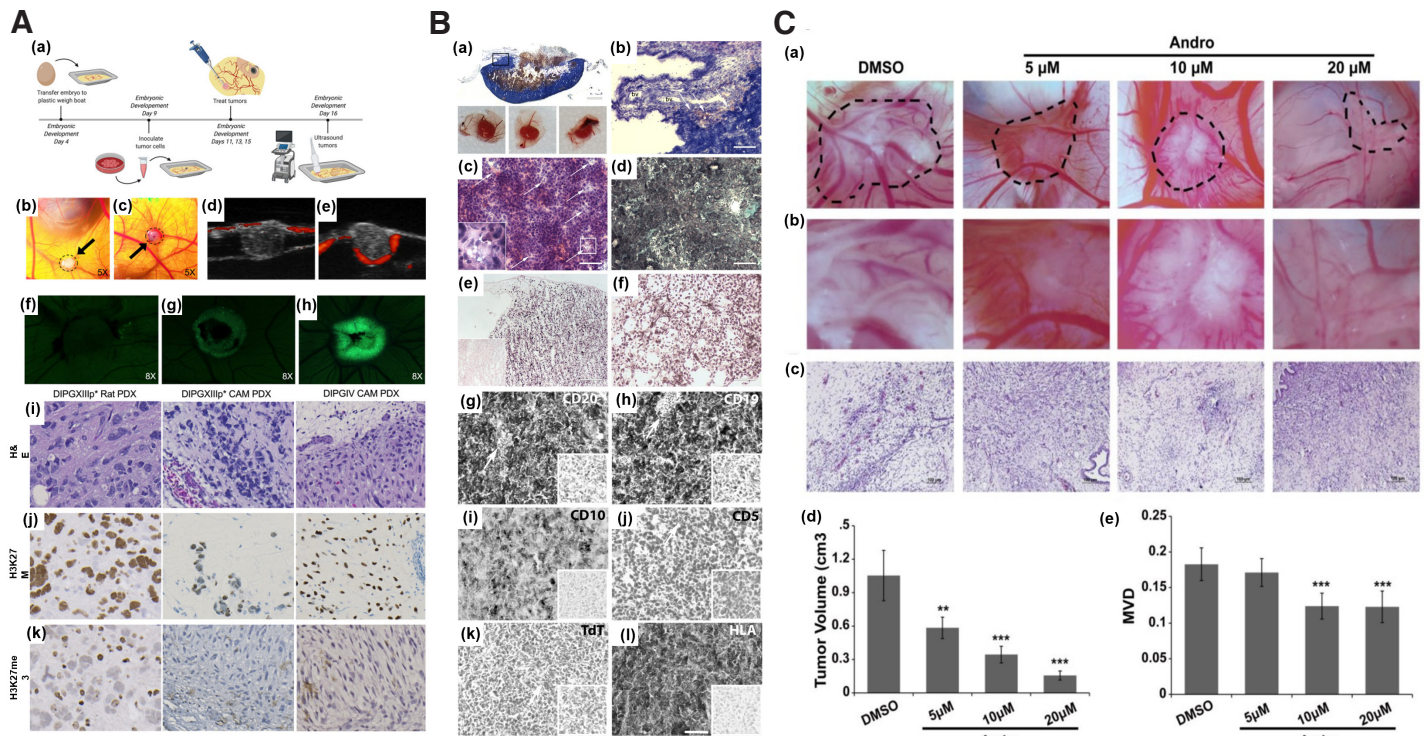


Fig. 2. The suitability of the chorioallantoic membrane (CAM) as a tumor-induced angiogenesis model. (A) Inoculation of patient-derived DIPG cell line on EDD9 (a); CAM DIPGIV (b) and DIPGXIIIp (c) xenografts at 48 h post inoculation; ultrasound image of DIPGIV (d) & DIPGXIIIp* (e) tumors grown below the CAM surface via RF power Doppler mode (red fluorescence represent active blood flow blood around the edges of tumor and within CAM; GFP tagged DIPGIV cells on CAM on EDD11 (f), EDD13 (g), & EDD15 (h); H&E and IHC staining of DIPGXIIIp* and DIPGIV tumors generated on rodent and CAM. Adapted from (Power *et al.*, 2022). **(B)** CAM BL2B95 tumor histology; Panoptic Pappenheim staining (a-b), H&E staining (c), Trichrome staining (d), Ki67 IHC staining (e), and Gomori silver staining (f). Adapted from (Klingenberg *et al.*, 2014). **(C)** Images and graphical representation of reduced tumor volume (a-b), and antiangiogenic activity of andrographolide (c-d); graphical representation of tumor volume (e). Adapted from (Dai *et al.*, 2017). All images are licensed under CC BY. Abbreviations: CAM, chorioallantoic membrane, DIPG, diffuse intrinsic pontine glioma; EDD9, embryonic development day 9; GFP, green fluorescent protein; H&E, Hematoxylin and Eosin, IHC immunohistochemistry.

heterogenous nature (Table 2). Though several methods of chick embryo culture have been described in literature, window method has been the most preferred culture technique for the screening of antiangiogenic agents or formulations using CAM standalone angiogenesis model.

3.2. CAM tumor xenograft as angiogenic model

Since 1990s, tumor xenografts have been successfully generated on CAM. Several types of tumor tissues have been grown on CAM with a high degree of correlation between the chick embryo assay and human tumors or mouse xenografts (Shoin *et al.*, 1991). Table 3 highlights the tumor xenografts generated in chick CAM models using different cell lines along with the outcome of the study in terms of the xenograft size, degree of angiogenesis and other histopathological features. The findings of available research indicate that vascular human tumor xenografts are reproducibly formed by employing chick microenvironments. Tumors of human melanoma, colorectal carcinoma and glioblastoma (GBM) cell lines grafted on the chick CAM successfully generated tumors of sizes 5-10 mm which recapitulated the hallmarks of corresponding human specimens (Durupt *et al.*, 2012). Diffuse intrinsic pontine glioma (DIPG) tumor grown on CAM exhibited similar genetic and epigenetic features as that of native tumors (Fig. 2A) (Power *et al.*, 2022). Burkitt lymphoma BL2B95 cell successfully generated on CAM showed a high degree of cellular, molecular and proliferative

similarity with the human disease (Fig. 2B) (Klingenberg *et al.*, 2014). Human ovarian OVCAR-8 xenograft exhibited close resemblance to cancer patient's tumor extracellular matrix (ECM), stromal cells and extensive vasculature that efficiently formed on chick CAM (Vu *et al.*, 2018). Hepatocellular carcinoma cell lines HUH7 and PLC/PRF/5 were grown with 100% success rate on chick CAM with an overall embryonic survival rate of up to 93% for HUH7 and 83% for PLC/PRF/5 using window method (Li *et al.*, 2015). Clear cell subtype of renal cell carcinoma, bladder and prostate cancer xenografts from established cell lines and freshly isolated patient-derived tissue were grown on CAM with $\geq 70\%$ success rate (Hu *et al.*, 2019). Similarly, eight osteosarcoma cell lines, HOS, MG63, HOS 143B, CAL-72, U2OS, MNNG-HOS, Saos-2 and UMR-106 were successfully generated on CAM (Kunz *et al.*, 2019). In view of the above studies, CAM tumor xenografts can be suitable model for studies targeted against tumor properties or therapeutics apart from antiangiogenesis including antineoplastic activity, drug assimilation and validation of active targeting strategies such as nanotechnology.

3.3. CAM tumor xenograft model for screening antiangiogenic compounds

Based on the robustness of the CAM model system, CAM xenografts have been employed for screening of anti-angiogenic compounds or lead molecules. Table 4 provides an overview of

recent studies that have used CAM tumor xenografts as models to evaluate potential inhibitors of tumor-induced angiogenesis. Tetrandrine at a concentration of 8 mg/ml (60 µl) exhibited decreased microvascular density (MVD) in CAM U87 xenograft (Ma et al., 2015b). Similar result of reduced blood vessel development was obtained with nobiletin (Chen et al., 2015), ruthenium(II)-p-cymene complexes (Nowak-Sliwinska et al., 2015), myricetin and galangin (Huang et al., 2015), theasaponin E1 (Li et al., 2021), theaflavin-3, 3'-digallate (Gao et al., 2016) in CAM ovarian adenocarcinoma xenograft. Ruthenium complexes showed significant decrease in the percentage of vascular network in breast cancer MDA-MB-231 xenograft bearing CAM (Guedes et al., 2020). Wogonoside showed decrease new blood vessel formation in breast cancer MCF-7 cell line in CAM (Huang et al., 2016). Andrographolide, at a concentration of 10-20 µM, was shown to inhibit breast cancer tumor growth and angiogenesis in CAM-bearing MDA-MB-231 cells (Fig. 2C) (Dai et al., 2017). As observed in CAM as standalone model

for angiogenesis study, amongst the several methods of chick embryo culture, window method has been the most commonly employed method for studies involving CAM tumor xenografts. This was followed by boat method and very limited information about the other methods.

3.4. Method of test compound administration on CAM model

CAM angiogenesis assay involves the application of the compounds to be evaluated onto the CAM. For this, the test compounds are generally loaded onto CAM surface using certain materials that can aid to localize and slowly but efficiently deliver the test compound into the underlying or surrounding CAM tissue. The commonly used materials in CAM standalone angiogenesis assay include sterile filter disc, gelatin sponge, coverslip, agarose, or matrigel. With sterile filter disc, the different concentrations of test compounds are generally loaded onto the disc by directly soaking it into the prepared test compound (Wang et al., 2015a).

TABLE 3 (PART 1/2)

REPRESENTATIVE STUDIES OF TUMOR XENOGRAPTS GENERATED IN CHICK CAM MODELS

Xenografted tumor type and cell line	Tissue/cell seeding density	Time frame	Outcome	Method	Reference
Alveolar rhabdomyosarcoma: RH30, CRL2061	1 × 10 ⁶ cells in 30 µl Matrigel	EDD8-EDD16	Solid tumors formed.	Window	(Pion et al., 2021)
Breast carcinoma: MDA-MB-231	2 × 10 ⁶ cells in 20 µl medium (50% Matrigel)	EDD7-EDD17	Xenografts established successfully.	Window	(Zuo et al., 2017)
Breast cancer: MDA-MB-231, breast cancer organotropic variants lung-metastatic (MDA-MB-231.LM2), bone-metastatic (MDA-MB-231.BoM) and brain-metastatic (MDA-MB-231.BRMS)	1 × 10 ⁵ to 1 × 10 ⁶ in 10 µl serum-free medium mixed with matrigel (1:1)	EDD9-EDD16	Displayed histological features (breast CSC markers CD44 & CD49f) similar to mice xenografts,	Window	(Pinto et al., 2020)
Burkitt lymphoma: BL2B95	1 × 10 ⁶ cells in 25 µl in BL medium mixed with Matrigel (1:1)	EDD10-EDD17	Xenografts with high degree of cellular, molecular & proliferative concord with human disease.	Window	(Klingenberg et al., 2014)
Chondrosarcoma cell line: SW1353	1 × 10 ⁶ cells in 100 µl Matrigel	EDD9-EDD16	Key features & IHC characteristics of native sarcoma tumors observed.	Window	(Sys et al., 2013)
Circulating cancer stem cells	Tumorspheres (diameter >50 µm) mixed with matrigel (total volume of 20 µl)	EDD8-EDD16	Recapitulate aggressiveness & proliferation capacity of native tumor.	Window	(Pizon et al., 2022)
Colorectal carcinoma: RKO	2 × 10 ⁶ cells in 25 µl serum-free DMEM	EDD15-EDD17	Xenografts (4-8 mm size) exhibited hallmarks of corresponding human specimens.	Window	(Crespo and Casar, 2016)
Colorectal carcinoma: HCT116	0.5 × 10 ⁶ cells in 25 µl serum-free DMEM	EDD15-EDD17	Xenografts (4-8 mm size) exhibited hallmarks of corresponding human specimens.	Window	(Crespo and Casar, 2016)
Canine osteosarcoma: D17	4 × 10 ⁶ in 15 µl of medium mixed with Matrigel (1:5)	EDD9-EDD14.5	Solid xenograft formed with induced angiogenesis.	Boat	(Ademi et al., 2021)
Canine oral melanoma: 17CM98	6 × 10 ⁶ in 15 µl of medium mixed with Matrigel (1:5)	EDD9-EDD14.5	Solid xenograft formed with induced angiogenesis.	Boat	(Ademi et al., 2021)
Colorectal: HCT 116	3 × 10 ⁵ cells in 20 µl Matrigel (1:1)	EDD9-EDD16	Viable tumors formed with feeder CAM vessels & various hypoxic zones.	Boat	(Harper et al., 2021)
Cutaneous T-cell Lymphomas: MyLa, SeAx	1 × 10 ⁶ cells in 25 µl RPMI 1640	EDD10-EDD17	Large 100-200 mg tumors formed.	Window	(Karagianni et al., 2022)
Diffuse intrinsic pontine glioma: DIP-GIV (H3.1K27M mutated), DIPGXIIIp (H3.3K27M mutated)	1 × 10 ⁶ cells in 10 µl Matrigel	EDD9-EDD16	Infiltrative & diffuse invasion behavior, showed positive H3K27M mutation similar to those in rodent.	Boat	(Power et al., 2022)
Epidermoid carcinoma: Hep3	0.4 × 10 ⁶ cells in 25 µl serum-free DMEM	EDD15-EDD17	Xenografts (4-8 mm size) exhibited hallmarks of corresponding human specimens.	Window	(Crespo and Casar, 2016)
Embryonal rhabdomyosarcoma: RD, TE671	1 × 10 ⁶ cells in 30 µl Matrigel	EDD8-EDD16	Solid xenografts formed with induced CAM angiogenesis.	Window	(Pion et al., 2021)
Esophageal adenocarcinoma: OE19	1 × 10 ⁶ cells in 20 µl medium	EDD7-EDD14	Xenografts of OE19 comparable to those in mouse.	Window	(Janser et al., 2019)
Fresh sarcoma-derived tumor tissues	10 ⁶ cells in 100 µl Matrigel	EDD9-EDD16	Vascularized xenografts exhibited key features of native sarcoma tumors.	Window	(Sys et al., 2013)
Fibrosarcoma: HT-1080	3 × 10 ⁵ cells in 20 µl Matrigel (1:1)	EDD9-EDD16	Xenografts with feeder CAM vessels & various hypoxic zones.	Boat	(Harper et al., 2021)
Fibrosarcom: HT-1080	0.5 × 10 ⁶ cells in 25 µl serum-free DMEM	EDD15-EDD17	Xenografts (4-8 mm size) exhibited hallmarks of corresponding human specimens.	Window	(Crespo and Casar, 2016)
Glioblastoma: U87	0.2 × 10 ⁶ cells in 25 µl serum-free DMEM	EDD15-EDD17	Xenografts (4-8 mm size) exhibited hallmarks of corresponding human specimens.	Window	(Crespo and Casar, 2016)
Glioblastoma: U87	1 × 10 ⁶ cells in 20 µl DMEN mixed with type I rat tail collagen (1:1)	EDD9-EDD12	Xenografts exhibited angiogenesis in spoked-wheel pattern.	Window	(Kavaliauskaitė et al., 2017)
Glioblastoma: U87	4 × 10 ⁶ in 15 µl of medium	EDD9-EDD14.5	Xenograft with angiogenesis.	Boat	(Ademi et al., 2021)
Glioblastoma: U87MG	6.0 × 10 ⁵ cells in 40 µl ice-cold Matrigel	EDD11-EDD14	Presence of necrotic area.	Window	(Mansur et al., 2022)

(Continued on the next page)

The size of the disc employed ranges from 2 mm (da Costa *et al.*, 2015) to 5 mm (Wang *et al.*, 2015a) in diameter. Similarly, for gelatin sponges (GS), implants of desired dimensions (example 1 mm³ size) are presoaked in different test compound and implanted onto CAM (Shah *et al.*, 2018) or the sponges are placed onto CAM and the test compounds are pipetted onto it (Ribatti *et al.*, 1997). GS have the benefit of being biocompatible or well tolerated by the embryos (Ribatti *et al.*, 1997). In addition, it adheres firmly to the CAM surface at the application site. In the case of coverslips, the test compounds are generally applied onto the coverslip, air-dried and placed onto CAM surface (Kim *et al.*, 2021). In terms of the size, sterile glass coverslip of 1 mm² are commonly used (Li *et al.*, 2016). Other methods include mixing of the test compounds with Matrigel or preparation in 1.2% agarose which could be directly applied onto the CAM surface (Lee *et al.*, 2017) or incorporated into disc which could be placed onto CAM (Samad *et al.*, 2018). Based on articles reviewed in our studies, sterile filter disc is the most

commonly employed material in the evaluation of the angiogenic property of novel compounds.

For efficient implantation of tumor cell lines onto CAM surface at a localized area, similar support materials as in CAM standalone angiogenesis assay have been used to load tumor cells onto CAM. According to review of literature in our study, Matrigel is the most commonly employed material for tumor cell implantation on CAM. With Matrigel, the cells to be implanted onto CAM are suspended into culture media mixed with Matrigel in different ratios (Zuo *et al.*, 2017). Matrigel as a cell carrier provides the ease to continuously visualize the test site (Lokman *et al.*, 2012). Silicon rings are also being commonly employed to keep the cells together on CAM surface (Kim *et al.*, 2021; Zuo *et al.*, 2017). The inner diameter of the silicon ring could range from 6 mm (Zuo *et al.*, 2017) to 9 mm (Kim *et al.*, 2021).

In CAM tumor xenograft models, the screening of antiangiogenic compounds is majorly performed by co-incubation of the

TABLE 3 (PART 2/2)

REPRESENTATIVE STUDIES OF TUMOR XENOGRAPTS GENERATED IN CHICK CAM MODELS

Xenografted tumor type and cell line	Tissue/cell seeding density	Time frame	Outcome	Method	Reference
Hepatoma: HuH7	5 × 10 ⁶ cells in 20 µl Matrigel	EDD7-EDD14	Xenografts of volume, 0.075 cm ³ or 0.69 cm ² obtained.	window	(Eckrich <i>et al.</i> , 2020)
Hepatocellular carcinoma: HUH7, PLC/PRF/5	5 × 10 ⁵ to 2 × 10 ⁶ cells in 40 µl of PBS++ and 20 µl of BM mixture	EDD10-EDD17	Vascularized xenografts & histological resembling those in mouse & undifferentiated HCC.	Window	(Li <i>et al.</i> , 2015)
Lung cancer: A549	3 × 10 ⁵ cells in 20 µl Matrigel (1:1)	EDD9-EDD16	Viable xenografts with feeder CAM vessels & various hypoxic zones.	Boat	(Harper <i>et al.</i> , 2021)
Malignant pleural mesothelioma (MPM)	Human tissue samples (fresh)	EDD7-EDD11	Xenografts with spoked wheel pattern of CAM arteries; exhibited biphasic features of metastatic human MPM cells.	Window	(Mindriřa <i>et al.</i> , 2017)
Melanoma: A375, SKMEL2	1 × 10 ⁶ cells in 25 µl serum-free DMEM	EDD15-EDD17	Xenografts (4-8 mm size) exhibited hallmarks of corresponding human specimens.	Window	(Crespo and Casar, 2016)
Melanoma: C8161	1 × 10 ⁶ cells in 30 µl PBS	EDD7-EDD14	Vascularized tumor xenografts formed.	Square Petri dish/boat	(Mangir <i>et al.</i> , 2018)
Melanoma: A375	1 × 10 ⁴ cells in 2 µl DMEM	EDD10-EDD17	Compact xenografts with mean surface area of ~1.5 to 2.2 mm ² .	Window	(Avram <i>et al.</i> , 2017)
Musculoskeletal system tumor (28 samples)	Samples of size 1-3 mm diameter	EDD9-EDD17	Tumor xenografts retained original tumor characteristics.	Window	(Sys <i>et al.</i> , 2012)
Multiple myeloma: OPM-2 ^{eGFP} , RP-MI-8226 ^{eGFP} spheroids	250,000 cells/spheroid with human bone-marrow mesenchymal cells (50,000 cells/ spheroid) in 30 µl drop of DMEM medium with collagen matrix (1:10)	EDD9-EDD14	Xenografts with angiogenesis in spoked-wheel pattern.	Boat	(Martowicz <i>et al.</i> , 2015)
Neuroblastoma: UKF-NB-4	5 × 10 ⁴ cells in 25 µl medium	EDD10-EDD14	UKF-NB-4 xenografts successfully established.	Boat	(Merlos Rodrigo <i>et al.</i> , 2021)
Neuroblastoma: UKF-NB-4	5 × 10 ⁶ cells in 25 µl medium.	EDD10-EDD17	UKF-NB-4 xenografts successfully established.	Window	(Merlos Rodrigo <i>et al.</i> , 2021)
Neuroblastoma: IMR32, BE2C	2 × 10 ⁶ in 5 µl of DMEM	EDD7-EDD14	Tumor xenografts of 1-5 mm size formed.	Window	(Swadi <i>et al.</i> , 2018)
Osteosarcoma: HOS, MG63, HOS 143B, CAL-72, U2OS, MNNG-HOS, Saos-2, UMR-106	1 × 10 ⁶ cells in 40 µl of medium mixed with matrix (1:1)	EDD9-EDD16	Solid xenografts comparable to those in rat.	Window	(Kunz <i>et al.</i> , 2019)
Osteosarcoma cells: Saos-2	1 × 10 ⁶ cells in 100 µl Matrigel	EDD9-EDD16	Vascularized xenografts exhibited key features of native sarcoma tumors.	Window	(Sys <i>et al.</i> , 2013)
Ovarian cancer: OVCAR-8-GFP	2 × 10 ⁶ cells in RPMI 1640 medium	EDD10-EDD	Xenografts masses exhibited close resemblance to cancer patient tumor with ECM, stromal cells & extensive vasculature.	Window	(Vu <i>et al.</i> , 2018)
Pancreatic: PANC-1	3 × 10 ⁵ cells in 20 µl Matrigel (1:1)	EDD9-EDD16	Viable xenografts with feeder CAM vessels & various hypoxic zones.	Boat	(Harper <i>et al.</i> , 2021)
Prostate carcinoma: PC3	1 × 10 ⁶ cells in 25 µl serum-free DMEM	EDD15-EDD17	Xenografts (4-8 mm size) exhibited hallmarks of corresponding human specimens.	Window	(Crespo and Casar, 2016)
Renal: Caki-1	3 × 10 ⁵ cells in 20 µl Matrigel (1:1)	EDD9-EDD16	Viable xenografts with feeder CAM vessels & various hypoxic zones.	Boat	(Harper <i>et al.</i> , 2021)
Prostate cancer PC3	1 × 10 ⁶ cells in 30 µl PBS	EDD7-EDD14	Vascularized tumor xenografts formed.	Square Petri dish/boat	(Mangir <i>et al.</i> , 2018)
Retinoblastoma: Y79 cells, eGFP Y79	2 × 10 ⁶ cells in medium with Matrigel	EDD7-EDD14	Xenograft formed Successfully.	Window	(Nair <i>et al.</i> , 2022)

[j] Abbreviations: BL-Burkitt lymphoma, BM-basement membrane, CSC-cancer stem cells, DIPG-Diffuse intrinsic pontine glioma, ECM-extracellular matrix, HCC-Hepatocellular carcinoma, IHC-Immunohistochemical, MPM-Malignant pleural mesothelioma, MV-microvascular endothelial.

test compound along with tumor cells at the time of xenografting (Ma *et al.*, 2015b). Another method employed for delivery of test compound to CAM tumor xenografts is the intravenous method (Nowak-Sliwinska *et al.*, 2015). Intravenous method has been employed in a limited way in preclinical CAM tumor models but is clinically most relevant.

4. Chick CAM as a model for antiangiogenic nanoformulation screening

Nanoparticles (NPs) in therapeutics have been attributed with several beneficial properties such as high biocompatibility, inertness, stability, efficient delivery to the target site, ability to integrate multiple therapeutic entities in a single NP formulation, enhanced imaging etc. (Garrier *et al.*, 2014). NPs employed for therapeutics based on the physical and chemical properties can be broadly divided into carbon, metal, ceramic (inorganic nonmetallic solids), lipid, polymeric and

semiconductor based (Khan *et al.*, 2019) (Fig. 3A). Carbon-based NPs for biological delivery and therapeutics include carbon nanotubes, carbon nano-onions, fullerenes, graphene and its derivatives, graphene oxide, carbon-based quantum dots, and nanodiamonds (Mahor *et al.*, 2021; Patel *et al.*, 2019). Most frequently used metal-based NPs for therapeutics include copper, gold, palladium, silver, titanium, and zinc NPs (Chandrakala *et al.*, 2022). Ceramic-based NPs for therapeutics include alumina, calcium phosphate, calcium carbonate, calcium sulfate, titania-based, tricalcium phosphate, hydroxyapatite, and bioactive glass ceramics (Kaushik, 2021). Polymeric NPs could be of natural or synthetic origin. Most commonly employed polymers for diagnostics, medical and pharmaceutical arena or biomedical application include synthetic polyethylene glycol (PEG), poly(lactic-co-glycolic acid) (PLGA), and polylactic acid (PLA) (Kaushik, 2021). Lipid-based NPs include liposomes, nanostructured lipid carriers, solid lipid NPs, and self-emulsifying drug-delivery systems (García-Pinel *et al.*, 2019). Semiconductor

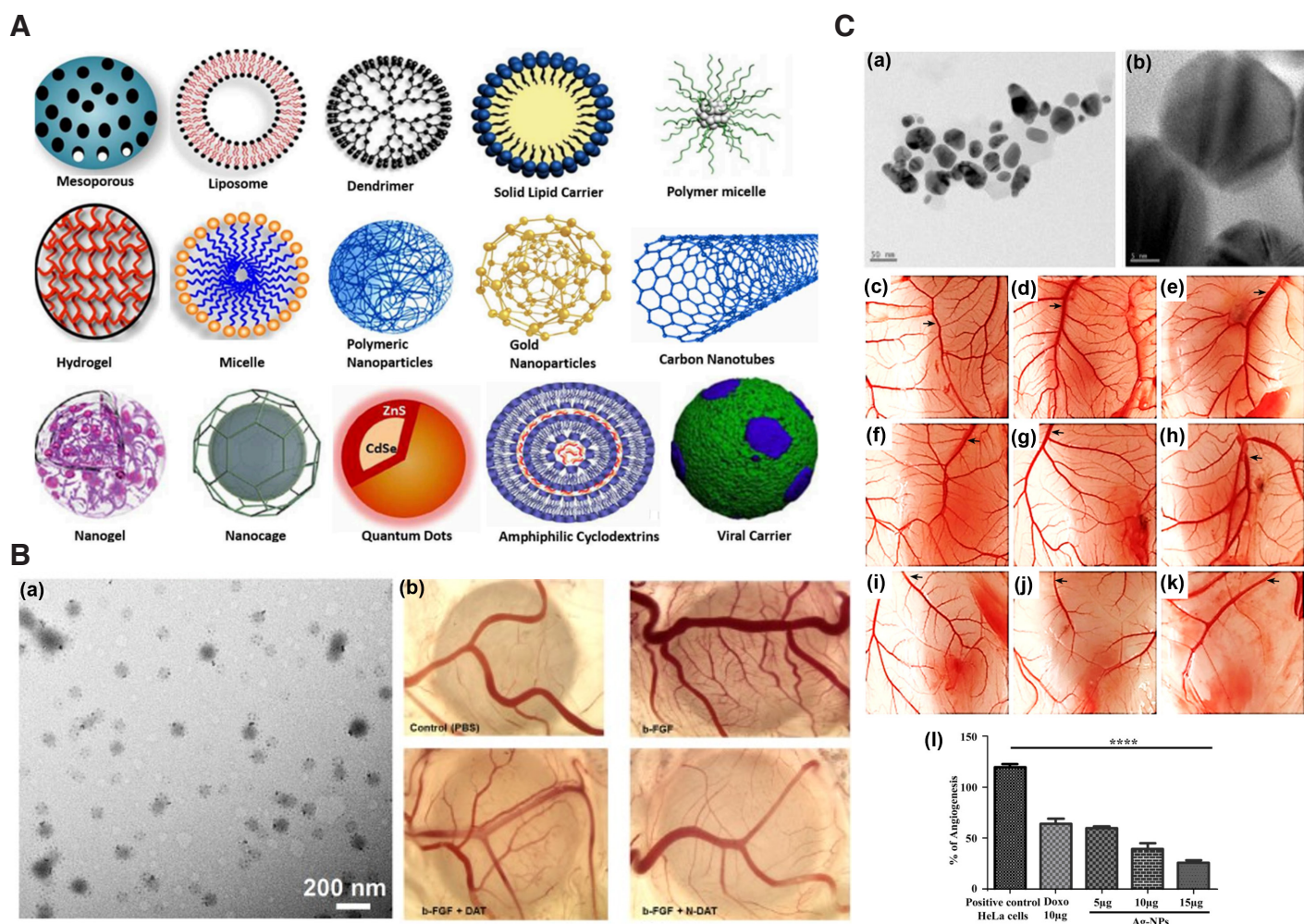


Fig. 3. Representative images of nanoparticles and their antiangiogenic activity in chick CAM. (A) Schematic representation of the different types of nanocarriers or NPs for drug delivery. Adapted from (Yaqoob *et al.*, 2020). (B) TEM image of NDAT (a); antiangiogenic activity of DAT and NDAT in bFGF-induced angiogenesis in CAM as a standalone model (b). Adapted from (Li *et al.*, 2019). (C) TEM images of silver (Ag) nanocomposite at 50 nm (a) & at 5 nm (b); images of CAM assay: untreated (c), treated with HeLa cells (d), treated with 10 µg/ml DOX (e), treatment with different concentrations of Ag nanocomposite in CAM alone (f-h) and CAM inoculated with HeLa cells (i-k). Graphical representation of angiogenesis inhibition by Ag nanocomposite (l). Adapted from (Pasha *et al.*, 2022). All images are licensed under CC BY. Abbreviations: CAM, chorioallantoic membrane; DAT, diamino propane tetraiodo-thyroacetic acid; DOX, doxorubicin; NDAT, DAT-conjugated PLGA nanoparticles; PLGA, poly (lactic-co-glycolic acid); TEM, transmission electron microscopy.

TABLE 4

REPRESENTATIVE STUDIES OF CHICK CAM TUMORS AS MODEL FOR SCREENING ANTIANGIOGENIC COMPOUNDS

Xenografted Human tumor cell line type	Antiangiogenic compounds	Nature of compounds	Treatment concentration	Effects on tumor angiogenesis	Reference
Glioblastoma: U87	Tetraandrine	Bis-benzylisoquinoline alkaloid	8 mg/ml (60 µl) in DMEM medium	↓ ratio of vascular & CAM area & MVD.	(Ma <i>et al.</i> , 2015b)
Ovarian adenocarcinoma: A2780	Nobiletin	Methoxyflavone	20 µM in 0.1 ml media + 0.1 Matrigel.	↓ BV development & tumor volume.	(Chen <i>et al.</i> , 2015)
Ovarian adenocarcinoma: A2780 cells as spheroid	Ruthenium(II)-p-cymene complexes	Organometallic	25-50 µM (80 µl) in 80 µl DMSO + 0.9% NaCl daily from EDD10-13	↓ angiogenesis & xenograft growth.	(Nowak-Sliwinska <i>et al.</i> , 2015)
Ovarian adenocarcinoma: OVCAR-3	Myricetin	Hexahydroxyflavone	20 µM in 20 µl medium + 80 µl Matrigel	↓ formation of BV.	(Huang <i>et al.</i> , 2015)
Ovarian adenocarcinoma: OVCAR-3	Galangin	Flavonol	40 µM in 20 µl medium + 80 µl Matrigel	↓ reduced formation of BV.	(Huang <i>et al.</i> , 2015)
Ovarian adenocarcinoma: OVCAR-3	Theasaponin E1	Oleanane-type saponin	4 µM in serum-free medium + Matrigel (1:4 (v/v))	↓ number & density of BV.	(Li <i>et al.</i> , 2021)
Ovarian adenocarcinoma: OVCAR-3	Theaflavin-3, 3'-digallate	Black tea phenolic	25 µM in 20 µl medium + 80 µl Matrigel	↓ BV development.	(Gao <i>et al.</i> , 2016)
Breast cancer: MDA-MB-231	Ruthenium complexes	Heterobimetallic	0.3-0.5 µM (50 µl) in DMSO + Hank's buffer at pH 7.4	↓ percentage of vascular network.	(Guedes <i>et al.</i> , 2020)
Breast cancer: MCF-7	Wogonoside	Flavonoid	50-200 ng/CAM saturated on sterilized filter paper disks (5 mm × 5 mm)	↓ new BV formation.	(Huang <i>et al.</i> , 2016)

[i] Abbreviations: BV-Blood vessel, C-Compound; MVD-micro-vessel density.

NPs such as quantum dots have been commonly used as probes in cells, tissues, or for membrane receptors (Walkey *et al.*, 2009).

Several physicochemical parameters of NPs including size, shape, surface chemistry and dosage, play pivotal roles in determining their suitability as effective and efficient therapeutics or drug delivery systems. Incidentally, it is now emerging that the biocompatibility and inertness of NPs though largely depend upon the chemical nature of the formulations, their particle size is one of the key factor that may influence the biological behavior of NP and this is now emerging to be the main problem associated with their unpredictable behaviors occasionally leading to nanotoxicity. NPs in the size range of 100-200 nm have good accumulation and retention rate at the tumor site but lesser penetrating ability within the tumor (Xu *et al.*, 2023). NPs in the size range of <70 nm have been considered to be most effective therapeutics or delivery system (Chauhan *et al.*, 2012; Jiang *et al.*, 2008), however, studies have shown NPs with sizes <70 nm to cause side effects (Mittal and Banerjee, 2016; Pan *et al.*, 2009). Additionally, certain NP size below the range of 10 nm can easily be eliminated as they have lower retention time within physiological system (Hoshyar *et al.*, 2016). These limitations in several instances have been overcome by techniques including green chemistry method or surface modifications. Gold nanoparticles (AuNPs) reported to be toxic (Pan *et al.*, 2009) when synthesized via a green chemistry approach using *Ganoderma* spp., were determined to be biocompatible. Surface coating of IONPs sized 5 and 30 nm with polymers such as PEG and carbohydrates such as dextran were observed to reduce porcine endothelial cell cytotoxicity (Yu *et al.*, 2012). In light of the aforementioned research findings, it is imperative to assess the potential toxicity of NPs alongside evaluating their efficiency and effectiveness in drug delivery. Given the extensive synthesis of diverse nanoparticles for medical applications, there is a pressing need for a comprehensive toxicity evaluation system with economical and quick read out. CAM models have demonstrated similarities to murine models in preclinical oncological studies and, in addition, offer economic advantages over murine models. To enhance the efficiency of nanotoxicity assessment, a parallel evaluation using a CAM system could be conducted, offering a cost-effective and expeditious method with reliable results.

4.1. Chick CAM standalone as an antiangiogenic nanotherapeutics model

Chick CAM standalone has proved to be a beneficial model for evaluation of anti-angiogenic properties of nanoformulations (Table 5). Silver NPs (AgNPs) synthesized using *Saliva officinalis* extract has shown significant dose-dependent reduction in hemoglobin content, number and length of the blood vessels in CAM standalone angiogenesis assay compared to control (Baharara *et al.*, 2014). Similarly, reduced angiogenic activity was observed in CAM with zinc oxide NPs synthesized using *Hyssops officinalis* L. extract (Fig. 3B) (Mohammad *et al.*, 2019). AgNPs coated with palm pollen extract (Homayouni-Tabrizi *et al.*, 2019), gold NPs (AuNPs) conjugated with KATWLPPR (Pedrosa *et al.*, 2017), molybdenum trioxide (Indrakumar and Korrapati, 2020), and magnetoliposomes loaded with thermosensitive betulinic acid (BA) (Farcas *et al.*, 2020) are other examples. Apart from CAM, yolk sac membrane (YSM) of the chick has been demonstrated to be beneficial for the evaluation of the angiogenic properties of NPs. The antiangiogenic activity of AuNPs conjugated with antiangiogenic peptides were exhibited in chick YSM (Roma-Rodrigues *et al.*, 2016). Using YSM (EDD3 to EDD5), PLGA NPs loaded with celecoxib were determined to exhibit antiangiogenic activity such as decreased blood vessels more significantly compared to the positive (NaCl) and negative (arginine) controls (Alonso-González *et al.*, 2022). The antiangiogenic activities exhibited in the aforementioned studies in CAM angiogenesis model were depicted as decrease in the number and length of CAM blood vessels, thickening of the blood vessel, capillary density, and inhibition of new blood vessel formation. The study period ranged from embryonic development day 3 to 12.

4.2. CAM tumor xenograft as antiangiogenic nanotherapeutics model

Tumor-bearing CAMs have not only proven to be an ideal model for screening antineoplastic agents but have also been employed for the screening of NPs and formulations for application in anti-angiogenic therapeutics (Table 5). Ag-NPs loaded with *Aspergillus niger* have been demonstrated to exhibit the antiangiogenic activity of reduced intercapillary network and blood vessel formation dose-

TABLE 5

NP AND FORMULATIONS WITH ANTI-ANGIOGENIC ACTIVITY EXHIBITED IN CHICK CAM

NP type	NP size	Dose	Model type	Experimental duration	Outcome	Reference
AgNP prepared using <i>Saliva officinalis</i> extract	1 – 40 nm	50, 100 & 200 µg/ml	CAM alone	8 th – 12 th day	↓ number & length of CAM BV; ↓ haemoglobin content dose dependently	(Baharara et al., 2014)
Gold NPs conjugated with KATWLPPR, (AuNPs@antiP)	Average diameter of 13 ± 2 nm	16.4 nM	CAM alone	3 rd – 4 th day	↓ new arteriole formation by 73%	(Pedrosa et al., 2017)
Gold NPs capped with polyethylene glycol 9000 & functionalized with camptothecin (AuNPs-PG9-CPT)	~180.5 nm	30 & 40 mg/ml (CPT=0.5mM)	CAM alone	4 th – 5 th day (24 h)	↓ BV branching	(Sadalage et al., 2021)
Artemisinin and dexamethasone-loaded nanodispersion	12 – 26 nm	50 µg	CAM alone	6 th – 7 th day	↓ branching & pre-existed BV	(Ponnusamy et al., 2019)
AuNPs conjugated with antiangiogenic peptides (P3–AuNPs).	13 ± 2 nm	40 µl (peptide conc.: 0.01 pmol/µl)	CAM alone	3 rd – 4 th day	↓ formation of new arterioles	(Roma-Rodrigues et al., 2016)
Magnetoliposomes loaded with thermo-sensitive BA	~200 nm	25 µM corresponding to BA conc.	CAM alone	7 th – 11 th day	↓ capillary density; hyperthermic pre-treatment samples caused embryo death	(Farcas et al., 2020)
Diclofenac incorporated PLGA NPs	Mean size of 150 nm	40 µl	CAM alone	4 th – 5 th day	↓ BV density	(Esteruelas et al., 2022)
Ag-NPs prepared using <i>Aspergillus niger</i>	8 to 55 nm	100 µl of 5, 10, & 15 µg/ml	CAM bearing HeLa cells	11 th – 14 th day	↓ intercapillary network and BV formation dose dependently	(Pasha et al., 2022)
Tetrac covalently linked to PLGA NP (Tetrac NP)	Average diameter of 200 nm	1 µg/CAM	CAM bearing h-RCC xenograft	7 th – 14 th day	↓ angiogenesis & subsequent reduction in tumor tumor growth.	(Yalcin et al., 2009)
Tetrac covalently link to PLGA NP (Tetrac NP)	Average diameter of 200 nm	1 µg/CAM	CAM bearing h-MTC xenograft	7 th – 14 th day	↓ haemoglobin content of xenograft; induced antiangiogenic thrombospondin 1 gene expression	(Yalcin et al., 2010c)
Tetrac covalently link to PLGA NP (Tetrac NP)	Average diameter of 200 nm	1 µg/CAM	CAM bearing FTC-236 tumor matrigel plug	7 th – 14 th day	↓ tumor mediated angiogenesis	(Yalcin et al., 2010b)

[j] Abbreviations: BA-Betulinic Acid, BV-Blood vessels, DAT-Diamino propane tetraiodothyroacetic acid, EC-Endothelial cells, FTC-236-Human follicular thyroid carcinoma, h-MTC-Human medullary thyroid carcinoma, h-RCC-human renal cell carcinoma, NP-Nanoparticles, PLGA-poly (lactic-co-glycolic acid), tetrac-Tetraiodothyroacetic acid, ↓-decreased/reduced.

dependently in CAM-bearing HeLa xenograft model compared to negative (PBS) and positive (doxorubicin DOX) control without NPs (Fig. 3C) (Pasha et al., 2022). Similarly, the antiangiogenic activity of drugs encapsulated with NPs, such as tetraiodothyroacetic acid (tetrac) covalently linked to PLGA (Tetrac NP), have been shown to inhibit the formation of new blood vessels in CAM-bearing xenografts of H1299 (Mousa et al., 2012), human RCC (Yalcin et al., 2009), h-MTC (Yalcin et al., 2010c), and FTC-236 tumor matrigel plug (Yalcin et al., 2010b). In addition, reduced hemoglobin content, elevated antiangiogenic thrombospondin 1 gene expression (Yalcin et al., 2010c) and subsequent reduction in tumor size compared to control and tetrac only (Mousa et al., 2012; Yalcin et al., 2009) as antiangiogenic characters on CAM tumor xenografts. These studies indicate the role of NP in the efficient delivery of antiangiogenic drugs that can be effectively examined by CAM tumor xenograft model.

4.3. Method of antiangiogenic nanoformulation administration in CAM model

The screening of nanoformulations as anti-angiogenic therapeutics using the CAM standalone model involves the delivery/application of test compounds employing similar techniques used in the screening of free test compounds (minus NPs) in CAM standalone angiogenic assay. The multi-walled nanotubes loaded with pachymic acid extract were applied to the CAM surface via 5 mm Waterman sterile filter paper (Ma et al., 2015a). Similarly, artemisinin and dexamethasone-loaded nanodispersion (Ponnusamy et al., 2019) and gold NPs capped with PEG 9000 functionalized with camptothecin (AuNPs-PG9-CPT) (Sadalage et al., 2021) were applied onto CAM via filter paper disc. For the evaluation of the

antiangiogenic therapeutic of AgNPs in CAM, the AgNPs were loaded onto GS, which were placed on the CAM surface (Baharara et al., 2014). The suitability of peptide-conjugated AuNPs as anti-angiogenic therapeutics in CAM was determined by placing within transparent plastic O-rings (6 mm diameter on the inside) placed on CAM (Pedrosa et al., 2017). Likewise, AuNPs conjugated with antiangiogenic peptides (P3–AuNPs) (Roma-Rodrigues et al., 2016) and magnetoliposomes loaded with thermosensitive BA (Farcas et al., 2020) were placed onto CAM within silicon/plastic O-rings placed on the vascularized CAM surface.

The antiangiogenic nanoformulation administration in CAM tumor xenograft model engages a similar technique as that of test compound in native form. Tetrac NPs at 1.0 µg targeted against renal carcinoma tumor angiogenesis growth were co-incubated along with 1×10^6 renal carcinoma cells in the medium mix with Matrigel (1:1 ratio) and xenografted on 7-day-old chick embryo CAM (Yalcin et al., 2009). Similarly, tetrac NPs were implanted along with respective tumor cells at the time of implantation on 7-day-old chick embryo CAM (Yalcin et al., 2010c). All these methods were effective in nanoformulation administration in CAM.

5. Comparison of CAM with other models used in antiangiogenic nanoformulation screening

There are several nanoformulations reported to have antiangiogenic properties. According to a review of literature of past 10 years using PubMed search driver with keyword, 'anti-angiogenesis nanoparticles', 139 articles with free full text solely concerned with studies on antiangiogenic nanoformulations were recorded as on August 2023. Out of 139 experimental outputs reported, 97 of the

studies were conducted in murine models, 71 in 2D models, 17 in CAM models, 4 in rabbit, 2 in zebrafish, and 1 in 3D model. Rodents and 2D cultures were the most commonly utilized angiogenic models for the evaluation of antiangiogenic nanoformulation delivery in biomedical research. 2D models comprised majorly of HUVECs (Babae *et al.*, 2014; Chuang *et al.*, 2019; Zhang *et al.*, 2021; Zou *et al.*, 2021), followed by other ECs such as: human endothelial somatic cell (EA.hy926) (Choi *et al.*, 2020; Lu *et al.*, 2020; Xing *et al.*, 2019), human retinal vascular ECs (hRVECs) and RF/6A (Sun *et al.*, 2023), telomerase-immortalized human microvascular endothelium (TIME) (Wang *et al.*, 2022a), primary human dermal microvascular ECs (Sheibani *et al.*, 2019), human retinal ECs (HRECs) (Shmueli *et al.*, 2013), human aortic ECs (HAEC) (Zhang *et al.*, 2017), rat retinal capillary ECs (Zeng *et al.*, 2019), and tumor cell lines including PC-3 (Son *et al.*, 2017) and PCa cells (Wang *et al.*, 2022b). Irrespective of the rationale behind engaging several or varied preclinical models for assessment of novel drug efficacy (Alphandéry, 2018; Shah *et al.*, 2019), only 10 out of 139 studies have engaged CAM and any other angiogenic model and can be useful to draw a comparison (Table 6).

Chick CAM has been in used for tissue growth purposes for hundred years but it remains underutilized for screening of antiangiogenic nanoformulations. Nevertheless, CAM has reestablished itself as a well-defined angiogenic model as evident from a series of studies where it has been in used in conjunction with other similar assays (Table 6). Discussed here are few studies that have employed CAM model along with 2D models. Zinc oxide NPs prepared using *Hyssops officinalis* extracts at a concentration of 12 µg/ml downregulated the expression of the key angiogenic genes VEGF and VEGF-R in the MCF7 breast cancer cell line, and in CAM they exhibited their antiangiogenic activity by reducing the number and length of blood vessels (Mohammad *et al.*, 2019). Similarly, electrostatically-conjugated bevacizumab-bearing dexamethasone-loaded poly(D,L-lactide-co-glycolide)/polyethylenimine NPs (eBev-DPPNs) exhibited antiangiogenic activity by decreased VEGF secretion in HUVEC and inhibited growth of new blood vessels in CAM leading to a decreased in blood vascular density (Liu *et al.*, 2019). Treatment of HUVECs with Mo polyoxometalates NPs (Mo POMs NPs) complex 3 at a concentration of 10 µg/ml exhibited interrupted sprouting or branching between tubes in 2D tube formation assay and significant inhibition of new blood vessel formation in CAM leading to reduction in the density or number of blood vessels (Zheng *et al.*, 2014). Silver NPs coated with palm pollen extract (Ag-PP NPs) downregulated the expression of pro-

angiogenic genes VEGF and its receptor VEGFR in MCF7 cells, which corroborated with CAM assay result of significant reduction in the number and length of blood vessels (Homayouni-Tabrizi *et al.*, 2019). Human breast cancer (MCF-7) cells treated with silver NPs coated with palm pollen extract (Ag-PP NPs) at a dose of 40 µM/ml for 10 h exhibited significant decrease in the expression of VEGF and VEGFR genes compared to the control. In the same study, antiangiogenic activity of Ag-PP NPs at a dose of 100 µM/ml was demonstrated in CAM via reduction in vessel length and branching (Homayouni-Tabrizi *et al.*, 2019). Docetaxel loaded NPs minus anti-FLT1 hexapeptide (DTX-loaded DBLaFLT1) treated HUVECs in tube formation assay exhibited significant decrease in the number of junctions, meshes, and master segments at a dose of 50 µg/ml which correspondingly exhibited antiangiogenic activity in CAM via reduced number of blood vessels in tumor (Conte *et al.*, 2019). Chondroitin sulfate conjugated to anti-Flt1-endostatin 2 NP (CS-ES2-AF NP) treated EA.hy926 cells at 50, 100, or 200 µg/ml exhibited dose-dependent suppression of their migration ability as well as inhibition of their tube formation ability at 200 µg/ml. Further, treatment of CS-ES2-AF NP at a concentration of 10, 25, or 50 µg/ml in CAM resulted in significant decrease in blood vessels in a dose-dependent manner (Xing *et al.*, 2019). Gold NPs conjugated quercetin (Qu) (at 50 µm of Qu and 195 µm of Au) treated HUVECs exhibited decreased cell viability, and significant reduction in the migration, invasion, and tube formation activity compared to free Qu. In addition, VEGFR-2 protein expression in HUVECs was significantly inhibited in comparison to free Qu. In the same study, investigation of anti-angiogenic property of Au NPs conjugated Qu in CAM exhibited anti-angiogenic activity of inhibiting new blood vessel formation (Balakrishnan *et al.*, 2016).

Some studies showed employment of CAM model in addition to 2D and murine models. Cetuximab-loaded copper sulfide NPs (CuS-Ab NPs) at a concentration of 10 µg/ml inhibited the viability and migratory ability of HUVECs. Similar antiangiogenic activity was observed in CAM and 4T1 xenograft bearing murine model on treatment with CuS-Ab NPs exhibited by reduced new blood vessel formation or reduction in blood vessel density, respectively (Li *et al.*, 2018). In another study, miRNA-7 loaded integrin-targeted biodegradable polymeric NPs exhibited antiangiogenic activity in HUVEC via reduction in cell viability, tube formation, 3D sprouting, and migration. In the same study, miRNA-7 loaded integrin-targeted biodegradable polymeric NPs demonstrated decreased vascular density between large blood vessels and reduced microvessel density or CD31 positive cells in CAM and subcutaneous neuro-

TABLE 6

NPs REPORTED TO EFFICIENTLY INHIBIT OR DELIVER ANTI-ANGIOGENIC AGENTS IN DIFFERENT PRECLINICAL MODEL SYSTEMS

Types of NPs	2D models	CAM	Murine model	Reference
Zinc oxide NPs prepared using <i>Hyssops officinalis</i> extracts	Yes	Yes		(Mohammad <i>et al.</i> , 2019)
Electrostatically-conjugated bevacizumab-bearing dexamethasone-loaded poly(D,L-lactide-co-glycolide)/polyethylenimine NPs (eBev-DPPNs)	Yes	Yes		(Liu <i>et al.</i> , 2019)
Mo polyoxometalates NPs (Mo POMs NPs) complex 3	Yes	Yes		(Zheng <i>et al.</i> , 2014)
Silver NPs coated with palm pollen extract (Ag-PP NPs)	Yes	Yes		(Homayouni-Tabrizi <i>et al.</i> , 2019)
Emodin-loaded magnesium silicate hollow nanocarriers (Emodin-MgSiO ₃)	Yes	Yes		(Ren <i>et al.</i> , 2014)
Docetaxel loaded NPs that do not bear anti-FLT1 hexapeptide (DTX-loaded DBLaFLT1)	Yes	Yes		(Conte <i>et al.</i> , 2019)
Chondroitin sulfate conjugated to anti-Flt1-endostatin 2 NP (CS-ES2-AF NP)	Yes	Yes		(Xing <i>et al.</i> , 2019)
Gold NPs conjugated quercetin	Yes	Yes		(Balakrishnan <i>et al.</i> , 2016)
Cetuximab loaded CuS NPs (CuS-Ab NPs)	Yes	Yes	Yes	(Li <i>et al.</i> , 2018)
miRNA-7 loaded integrin-targeted biodegradable polymeric nanoparticles	Yes	Yes	Yes	(Babae <i>et al.</i> , 2014)

[i] Abbreviations: CAM-Chorioallantoic membrane, NP-Nanoparticles, 2D-Two-dimensional, 3D-Three-dimensional.

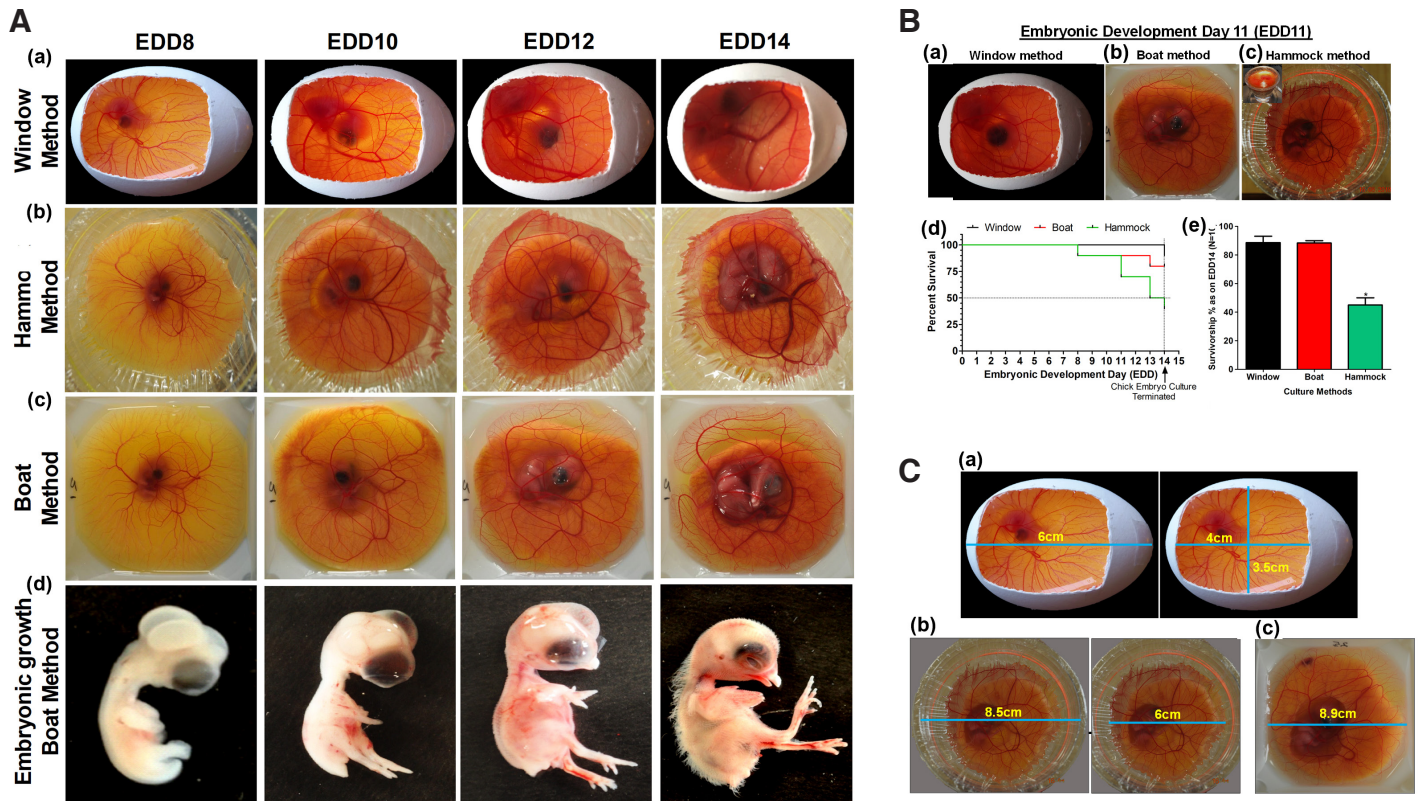


Fig. 4. Chick embryo culture techniques. (A) Timeline of chick embryo development and CAM vasculature. All the systems, window (a), hammock (b) and boat (c) exhibit similar patterns of CAM angiogenesis with differential survival in a climate-controlled humidity chamber; embryos dissected (d) from these indicate that HH (Hamburger-Hamilton) developmental milestones are attained in a temporal fashion. All embryos appear healthy; interestingly unhealthy embryos die overtime. (B) Relative survivorship comparison of the three models of CAM culture technique. (B a-c) Representative images of developing chick embryo on EDD11 of embryogenesis in (a) window method, (b) boat method and (c) hammock method; (d) Kaplan-Meier survivorship curve of embryos grown using these methods; (e) graphical representation of the differential survival percentage at the end of EDD14; n=10 for each method. Data is represented as mean \pm standard deviation. For comparison of means, one-way ANOVA followed by post-hoc Tukey's multiple comparison analysis was performed. * $p < 0.05$ indicates statistically significant differences. (C) Chick CAM surface area for experimental manipulation: (a) window method showing dimensions for experimental manipulation and visualization; similarly, (b) hammock and (c) boat methods are indicated. The dimensions indicated here are at their maximum limit as per our study. Images: Nikon 5100 DSLR camera.

blastoma (N2A) xenograft bearing mouse model, respectively (Babae *et al.*, 2014).

The above studies clearly indicate strong analogy of CAM model to other fundamental angiogenesis models, thereby, their reproducibility and suitability as a model for the screening of antiangiogenic nanoformulations.

6. Practical illustration of chick CAM model to study angiogenesis and NPs as a therapeutic carrier

6.1. Chick embryo culture with CAM genesis

Out of several methods described in the literature, windowing, cling-wrap hammock and polystyrene boat are simple, sustainable and flexibly fit into the scope and requirements of any experimentation. To assess the advantages of one method over others, we have demonstrated and compared the developmental timeline and outcome of chick embryos for polystyrene weigh boat, windowing, and cling-wrap hammock method (Fig. 4A). After calibrating different conditions reported in literature, temperature of $37^{\circ}\text{C} \pm 1$ and relative humidity (RH) $\geq 80\% \pm 10$ was observed to

be crucial for normal development of blood vasculature as well as chick embryo. Both qualitative and semi-quantitative observations of images captured indicate CAM to be highly vascularized, transparent, easy to visualize with or without microscope. In addition, temporal and spatial patterns of blood vessel formation and distribution remain more or less constant among different embryos. CAM exhibited similar pattern of vascularization across the cultures, with no distinct morphological abnormality in embryos indicating the suitability of the set methods/conditions adopted. Survivorship curve plotted for three widely used techniques of *ex ovo* or *in ovo* culture at optimal temperature and humidity clearly indicated selective advantage of windowing and polystyrene boat method over cling-wrap hammock in a climate-controlled chamber (Fig. 4B). Of the three culture methods, polystyrene boat method was observed to have a significant advantage over the other two methods in, a) survivorship over 14-days (only against cling-wrap hammock method), b) larger area of CAM for manipulation (Fig. 4C), c) easy to capture image under dissecting microscope. The available surface area for manipulation in boat method was determined to be $\sim 79.2\text{cm}^2$, hammock $\sim 28.27\text{cm}^2$, and windowing

~14cm². In future, this setup can be manipulated to perform live fluorescence imaging (Nowak-Sliwinska *et al.*, 2010; Smith *et al.*, 2007) without needing many attachments.

6.2. Chick CAM as an anti-angiogenic model

Angiogenesis is an important hallmark of tumor cells, a requisite route for gases and nutrient supply as well as metastasis. Targeting angiogenesis is considered to be a potentially effective approach for the treatment of cancer (Zhao and Adjei, 2015). To substantiate chick CAM as an ideal anti-angiogenic model, doxorubicin (DOX) (Uvez *et al.*, 2020) and Irinotecan (IRT) (Bocci *et al.*, 2008) previously reported to have an anti-angiogenic property were used for demonstration. Qualitatively CAM exhibited vessel disorganization, bending or looping, in response to different dosages of DOX and IRT concentrations. Quantitatively, around the vicinity (within 1.5 cm × 1.5 cm area) of DOX and IRT administration, CAM exhibited lesser vascular density compared to vehicle (1×PBS) treated sites which was determined by measuring important parameters like the number of nodes, meshes and total branching length using angiogenesis analyzer tool add-on to ImageJ version 1.52a, (National Institute of Health, Bethesda, MD, US). A reduction in blood vascular density compared to vehicle (1×PBS) treated sites was observed, indicating

the antiangiogenic potential of the administered dose of DOX (Fig. 5A) and IRT (Fig. 5B).

6.3. CAM tumor xenograft growth and angiogenesis assessment

Extensive vascular bed and innate immunodeficiency till EDD14 provide a conducive environment for engraftment of human tumor cell lines. Corresponding to earlier work (Kunz *et al.*, 2019), implantation of U87 GBM cells at a density of 7.5×10^5 to 1.5×10^6 on EDD8/9 consistently gave rise to highly vascular tumors of sizes ranging from 0.75 – 4.2 mm³. Implantation on EDD7 were often associated with reduced tumor growth success and increased mortality of the embryos. On EDD7, CAM is usually small and does not grow sufficiently beyond amniotic depression, therefore tumor loaded gelatin sponge (GS) often depressed and lead to death of the embryo. Tumor cells implanted on 10th or 11th day resulted in smaller tumor xenografts as experiments were bound to terminate at EDD14 to prevent variability that might arise due to infiltration of immune cells and ethical concerns. Since only tumor cells are implanted onto CAM, it appears that U87 cells recruit chick endothelial, fibroblasts and secrete ECM to form solid xenograft. ECs can be observed as profuse blood vessels in the histological sections photographed at 100 and 400 magnification (× 10 and × 40 objective) (Fig. 6A).

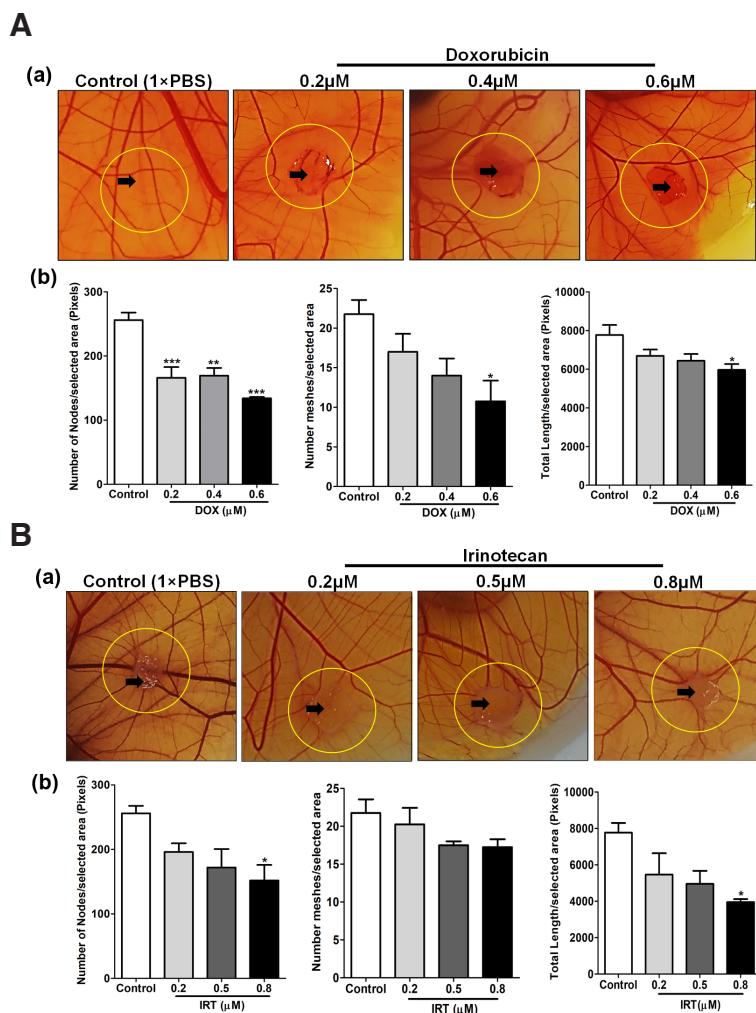


Fig. 5. Anti-angiogenic properties of DOX and IRT at various dosages. (A) Photographic representation (upper row) and quantitative analysis (lower row) of anti-angiogenic properties of DOX at various dosages (0.2, 0.4 & 0.6 μM) and control (1×PBS). Treatment was given on EDD9 and incubated for 48 h. Images captured through Nikon DSLR were analyzed for macrovascular organization by quantifying nodes, meshes and the total length of blood vessels around the site of drug administration using the ImageJ version 1.52a angiogenesis analyzer plugin. **(B)** Photographic representation (upper row) and quantitative analysis (lower row) of anti-angiogenic properties of Irinotecan at various dosages (0.2, 0.5 & 0.8 μM) and control (1×PBS). Treatment was given on EDD9 and incubated for 48 h. Images captured through Nikon DSLR were analyzed for the macrovascular organization by quantifying nodes, meshes and the total length of blood vessels around the site of drug administration using the ImageJ version 1.52a angiogenesis analyzer plugin (n=5). Statistically, analysis indicates a significant decrease in the nodes in the treated compared to control. Overall dose-dependent reduction in the nodes, meshes and length of blood vessels was observed. Statistical analysis was done using GraphPad Prism-5 software, San Diego, CA. All the data are represented as mean ± standard deviation. For comparison of means, one-way ANOVA followed by post-hoc Tukey's multiple comparison analysis was performed. *p<0.05, **p<0.01, ***p<0.001 indicate statistically significant difference.

6.4. Distribution of NPs in CAM U87 xenograft growth

As proof of concept, accumulation of IONPs of <50 nm and 50-100 nm sizes were determined post systemic injections in developing xenograft. Histological examination confirms that these particles were observed to be localized intracellularly as well as extracellularly within cells of xenograft (Fig. 6B). Intravenously administered NPs seems to remain in circulation and accumulate within tumor xenograft overtime. Here, variable size IONPs were used to investigate the impact of size on its ability to distribute within tumor tissue. Qualitatively, results indicate passive accumulation of <50 nm particles to be higher in comparison to 100 nm particles. Additional work will be performed with surface coated IONP and observe its accumulation within tumor tissue. Reproducibility, ease of manipulation, budget and quality data obtained through experimentation will certainly make this model an alternative to performing nano-characterization experiments.

6.5. Protocol for CAM angiogenesis and NP characterization

6.5.1. Chick embryo culture

Pathogen-free fertilized white Leghorn (*Gallus gallus*) eggs were procured from Venky's (India) Limited, Haryana Division, India. Eggs were wiped with alcohol 70%, numbered, weighed, and placed inside a humidified chamber (REMI CHM-10 PLUS) in a horizontal position for incubation at $37^{\circ}\text{C} \pm 1$ and $80\% \pm 10$ relative humidity. The eggs were rotated after every 3-4 h during the daytime to prevent the vitelline membrane from sticking on to the eggshell until the preparation of the culture for experimental manipulation. This study was approved by the Institutional Animal Ethics Committee (IAEC approval; ID DU/KR/IAEC/2017/06).

Windowing method (in ovo): Briefly, on EDD3, HH (Hamburger and Hamilton) stage 20, a hole was made on the narrower end side of

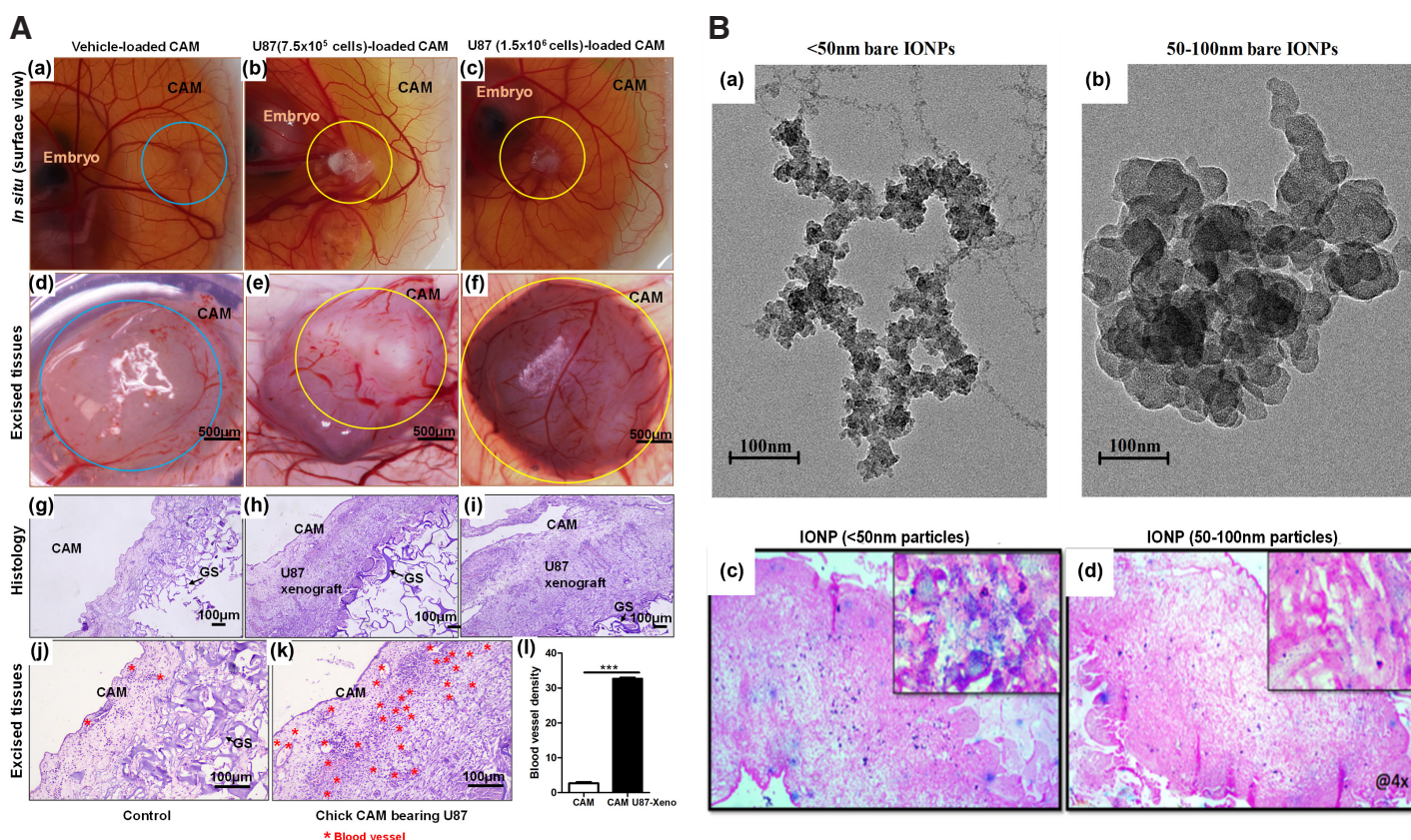


Fig. 6. Images of CAM U87 xenografts and distribution of IONPs within the tumor. (A) (a-l) CAM U87 xenografts 6 days (EDD9-EDD15) post inoculation. **(a-c)** *In situ* images of chick CAM implanted with different U87 cell densities and control with only the media; **(d-f)** corresponding excised explants of a-c vertically imaged under Radical Stereo Zoom Microscope fitted with a camera; **(g-i)** histological sections (H&E staining) of corresponding explants of d-f vertically imaged with the help of Nikon Eclipse Ts2R microscope; **(j,k)** higher magnifications. **(l)** Qualitative image analysis of histology indicates numerous small blood vessels and capillaries along with tumor cells. The compactness of the solid tumor indicates that apart from tumor and endothelial cells, other supporting cells were also recruited within the U87 xenograft. Circles represent the site of transplants/explants; blue circles represent GS minus tumor cells; yellow circles represent U87 xenografts. The black arrow indicates vascular structure (n=3). The blood vessels were counted under brightfield imaging at a 200 magnification (x20 objective) in 3 fields with high blood vessel density. The data is represented as mean \pm standard deviation. For comparison of means, a two-tailed unpaired t-test was performed. ***p<0.001 indicates statistically significant differences. **(B) (a,b)** Transmission electron microscopy images of IONPs. **(c,d)** Images captured at low magnification to observe overall accumulation and 100 \times insets demonstrate intracellular localization of IONPs. Images show accumulation of bare IONPs <50 nm and 50-100 nm injected systemically on EDD14. Six hours post-injection of IONPs into CAM blood vessels, xenografts were excised and processed for paraffin embedding and histology. Prussian blue pigments on the 5 μm sections qualitatively indicate that <50 nm particles efficiently accumulate within the xenograft. The image was taken with Nikon Eclipse E200 upright brightfield microscope. Abbreviations: CAM, chorioallantoic membrane, EDD, embryonic development day; GS, gelatin sponge; IONPs, iron oxide nanoparticles.

the egg and 4 ml of albumin was removed to prevent developing CAM from sticking onto eggshell. On EDD4 (HH stage 24), 1.5 × 1.5 cm to ~3 × 2.5 cm window (determined on the need of the experiment) was created for easy access or visualization of developing embryos. The window is then sealed with a sterile breathable parafilm strip and replaced inside the Humidity chamber.

Shell-less culture (ex ovo) technique: For the boat and hammock method, eggs were opened on the EDD4 (HH stage 24) and contents transferred in the polystyrene square weigh dish/boat (3.5 L x 3.5 W x 1 Depth, in inches; Cole-Parmer Instrument Co.) or hammock, made with the help of normal food cling wrap supported by plastic juice cup. The plastic cup was filled with sterile water to stabilize the assemblage. The polystyrene boat culture dishes were sealed with parafilm and the cling-wrap hammocks covered with the plastic juice cup caps and placed in trays kept inside the humidity chamber. Growth of embryos was monitored from time to time for its health.

6.5.2. Chick CAM angiogenesis assay

On EDD9 (HH stage 34), GS of approximately 6.6 mm x 6.6 mm x 3.5 mm (L x B x thickness), pre-soaked overnight in test compounds (60 µl) were implanted onto the CAM. On EDD11, images were taken of the chick CAM and the vascularization network analyzed with ImageJ for the quantitative determination of the anti-angiogenic effect of the test compounds through the number of nodes, meshes and total length formed.

6.5.3. GBM-xenograft growth on CAM

25 µl of cell suspension with a cell density of about 750,000 to 1.5 × 10⁶ U87(MG) cells were loaded onto GS (L x B, 4 mm x 4 mm; thickness, 2 mm) and placed on chick CAM of EDD9 (HH stage 34). To maintain uniformity, sponges were placed in the area of minor vascular branches with the cell suspension side facing the CAM surface. The chick embryos with grafted U87 cells were then placed in the humidity chamber maintained at optimized conditions of 37°C ± 1 and 80% ± 10 humidity. On EDD14, the tumor xenografts were excised with the help of dissecting scissors and forceps. Measurements were taken with a caliper for volume calculation. Volumes were calculated using the equation: volume (mm³) = (W² × L)/2, where, L = major anteroposterior diameter, W = diameter from left to right (Tomayko and Reynolds, 1989).

6.5.4. Analysis of tumor-induced CAM angiogenesis

For this study, U87 xenografts were fixed overnight in 10% formalin and processed for hematoxylin and eosin (H&E) staining following the standard protocol. The xenografts were dehydrated and cleared by passing through a series of graded alcohols in the order: 10 > 70 > 80 > 90 > 100% > acetone > xylene 2× each for 20 minutes. This was followed by tissue embedding which involved placing of the specimen in wax-filled molds 2× maintained at 70°C for 20 minutes. The specimen block was then allowed to solidify on a cool surface and when set, the mold was removed. The block containing the specimen was trimmed and sections of 4 µm were cut with steel blades. Sections are then floated out on the surface of warm water (50°C) in a tissue floatation bath to flatten them and picked onto microscope slides. After thorough drying, the tissue slides were process for staining. Staining involved the following steps in the indicated order: warming of slide at 70°C for 5

minutes > clearing of wax from tissue sections with xylene 2× for 3-5 minutes each > acetone 2× for 2-3 minutes each > thorough washing in running tap water for 5 minutes > staining the slide with Harris hematoxylin nuclear stain for 1 minute > one dip in 1% acid alcohol > rinsing in running tap water > staining with an aqueous or alcoholic solution of eosin for 30 seconds > passing of the slide through several changes of alcohol to remove all traces of water > rinsed in several baths of xylene > application of a thin layer of polystyrene mountant (DPX-Dibutylphthalate Polystyrene Xylene) > glass coverslip covering. The prepared stained tissue sections were then evaluated for blood vessels.

6.5.5. Injection of nanoparticles

Chick CAM of EDD14 bearing tumor xenograft were intravenously injected with about 50 µl of IONPs dissolved in 1×PBS (0.61 mg/ml) with the help of an Insulin syringe (Dispo Van U-40 Insulin Syringe). 5-6 h post-inoculation, the tumor xenografts were excised and tissue sections of Prussian blue (PB) pigments by iron-Prussian blue reaction were prepared for the determination of IONP distribution/localization. Briefly, following deparaffinization and hydration of the tissue slide (passing through a series of alcohols in the order: 100 > 95 > 90 > 80 > 70 > distilled water for 3-5 minutes in each), a mixture of 2% HCl and 2% ferrocyanide in equal parts were placed on the slide and kept at room temperature (RT) for 30 minutes. The slide was washed with distilled water and incubated with nuclear fast red for 5 minutes at RT. After which, the tissue slide was washed several times with tap water and distilled water. This was followed by dehydration with a series of alcohol in the following order: 70 > 80 > 90 > 95 > 100%. The slide was then mounted with DPX and covered with a coverslip.

7. Advantages and limitations of CAM as a 3D model for tumor angiogenesis and nanotherapeutics evaluation

Compared to other methods, the CAM is an easy, swift, and inexpensive biomedical research model. The chick embryo can receive transplants from different tissues and animals without developing an immune reaction. Murphy transplanted different tissues into adult and embryonic chickens to answer immunological questions for the first time. He then demonstrated that while rat tissues could not be sustained in adult chickens, they could grow on the CAM until day 18 of development (Murphy, 1914).

The chick CAM can successfully support tumor growth with the majority of retention of cancer cell characteristics, such as growth, invasion, angiogenesis, and remodeling of the microenvironment, due to an immature immune system. Additionally, the sequencing of the chicken genome showed a high degree of sequence similarity to humans.

The biggest drawback of CAM assays is a non-specific inflammatory response, which might happen if experiments are run past the recommended 15-day incubation period. A non-specific inflammatory response is substantially less likely when the tissue is transplanted as soon as the CAM begins to grow and the host's immune system is relatively young (Leene *et al.*, 1973). The timing of the CAM angiogenic response is crucial because real neovascularization is difficult to differentiate from an erroneously enhanced vascular density caused by rearranging existing arteries (Knighton *et al.*, 1991). Another limitation of the CAM model is the limited time to perform the experiments (generally limited to a week). The short

time window hampers the detection of metastasis to secondary sites. In addition, the CAM is highly susceptible to environmental modifications, including variations in oxygen tension, osmolarity, pH, and the degree of keratinization (Auerbach et al., 1974).

8. Ethical considerations

Considering the widespread concern over the extensive usage of murine models, the cost, the pain and the suffering they endure in the process, WMS Russell and RL Burch proposed in 1959 the 3R strategy which stands for *replacement* of highly sensitive higher organisms with impervious forms, *reduction* of the number of organisms used to obtain the desired result, and *refinement* to reduce the inhumane practices endured by the animal model during experimentation (Tannenbaum and Bennett, 2015). The proposal was to refine the welfare of research animal models or find an alternative model but at the same time without compromising on the quality of biomedical research findings.

The murine models posed a disadvantage when it comes to the 3R strategy proposed by Russell and Burch (1959) to lessen the sufferings on experimental animals. More concerning is the fact that most of the preclinical studies undertaken using murine models are expensive and time-consuming. This void could be easily bridged by using the CAM model, before moving on to murine models for further validation, thereby aiding in reducing the usage of murine models.

Unlike murine models, the usage of the CAM model in biomedical research is considered to be associated with lesser restrictions. In several places, the usage of CAM does not require any ethical clearance, while in others, a simple protocol approval by the concern committee or a definite review as that for vertebrate animal procedure dependent on the intended stage of the embryo for experimental use is required. According to the Office of Laboratory Animal Welfare (OLAW), National Institute of Health (NIH), US, avian embryos are considered live vertebrate animal only on hatching, therefore, omitting the hassles of ethical approval prior to use of avian embryonic stages (Robl et al., 1991). OLAW is a division of the NIH which develops, implements and oversees the compliance on the Humane Care and Use of Laboratory Animals (Policy) with that of the Public Health Service (PHS) Policy. On account of the general agreement in the scientific community on the probable development of sufficient perception by chick embryos past two thirds of their incubation/developmental period (day ≤ 14 in the case of avians with a total incubation period of 21 days), it is highly recommended that research institutions or their parent bodies have a set rule of policies and procedures or an Institutional Animal Care and Use Committee (IACUC) to address the care or euthanasia of animals, including avian embryos. At Brown University, one of the oldest institutes of higher education in the United States, the IACUC guideline undermines the need for IACUC review for studies involving avian embryos of day ≤ 18 (Brown University, 2019). In Boston University, in accordance to the Office of Research, usage of embryos before day 16 of incubation does not require prior approval from IACUC, however, it is recommended of the principal investigator to submit a letter to the IACUC stating briefly the experimental procedure using the embryonated eggs (Boston University, 2023). University of Illinois Urbana-Champaign IACUC follows a similar policy as that of Boston University on the use of avian embryo,

i.e., presentation of complete experimental procedure to IACUC (Illinois Urbana-Champaign, 2023). The directive 2010/63/EU of the European Parliament and the council of 22 September 2010 on the protection of animals used for scientific purposes emphasizes on a similar principle that non-mammalian embryonic forms before the first two thirds of their developmental stage could be employed without any restrictions, i.e., chick embryos of day ≤ 14 (European Parliament & Union, 2010). In India until June 2023 no approval was required for use of avian embryos for experimental purpose, however, beginning 5th June 2023, based on the Committee for the Purpose of Control And Supervision of Experiments on Animals (CCSEA) notification, a protocol approval is required from institutional animal ethics committee (IAEC) (CCSEA, 2023). In view of the above information, studies using chick embryo across the globe are govern by similar IACUC or animal protection for scientific purpose policies.

9. Conclusion

The literature strongly suggests the use of chick CAM as one of the advantageous pre-clinical alternative to the animal-based murine model. However, on a different note, it is clear that a single *in vivo* model is insufficient to fully understand the process of angiogenesis. Thus, having data from CAM in addition to emerging and conventional model (murine, rabbit, zebrafish, aortic ring, choroid, and 2D) will provide a strong rationale and support for taking the lead molecules/nanoformulation to next level validation in higher animal. Efforts should be made to popularize simple economical systems and accelerate drug discovery research as well as simultaneously reduce the number of higher animals used in cancer and angiogenesis research.

Acknowledgments

We are thankful to Prof. Savita Roy, Principal, Daulat Ram College, University of Delhi for providing constant support and lab facility throughout the investigation. We also thank Zebrafish Lab Facility, Daulat Ram College, for the use of the Radical Stereo Zoom Microscope.

Ethics approval and consent to participate

This study involving chick embryos was carried out at the Neuropharmacology and Drug Delivery Laboratory, Zoology Department, Daulat Ram College, University of Delhi and was approved by the IAEC of Kirori Mal College, University of Delhi (IAEC approval ID DU/KR/IAEC/2017/06). In the study, embryonic development was strictly terminated by day 14 (EDD14) to comply with the 3R requirement and avoid ethical violations.

Availability of data and materials

The data sets used and or/analyzed during the current study are available from the corresponding author upon reasonable request.

Competing interests

The authors declare that no competing interests exist.

Funding

Financial support from Indian Council of Medical Research (ICMR-ICRC) (No.5/13/4/ACB/ICRC/2020/NCD-III), Institution of Eminence, University of Delhi (Ref. No./IoE/2023-24/12/FRP), ICMR AdHOC (2021-10573/GENOMIC/ADHOC-BMS) to ACB is thankfully acknowledged. The study was partly supported by Senior Research Fellowships to TT (764/

(CSIR-UGC NET JUNE 2019) and AC [573/(CSIR-UGC NET JUNE 2017)] by the University Grants Commission (UGC); Senior Research Fellowships to NA (09/045(1622)/2018-EMR-I), JY (09/045(1629)/2019-EMR-I) and DJ (09/0045/(11635)/2021-EMR-1) and a Junior Research Fellowship to AC (09/0045(12901)/2022-EMR-1) by the Council of Scientific and Industrial Research (CSIR).

Author's contributions

Conceptualization: ACB; Data curation: AS, TT, DJ, SKY, ACB; Formal analysis: AS, TT, DJ, SKY, NA, JY, AC, AC, UJ, PS; Funding acquisition: ACB. Investigation: AS, TT, DJ, SKY, ACB. Methodology: AS, TT, DJ, SKY, NA, JY, AC, AC, UJ, PS; Project administration: ACB; Resources: ACB, AS; Supervision: ACB; Validation: ACB; Visualization: AS, TT, DJ, SKY, ACB; Writing original draft: AS, ACB; Review and editing: ACB.

References

- ADEMI H., SHINDE D. A., GASSMANN M., GERST D., CHAACHOUAY H., VOGEL J., GORR T. A. (2021). Targeting neovascularization and respiration of tumor grafts grown on chick embryo chorioallantoic membranes. *PLoS ONE* 16: e0251765. <https://doi.org/10.1371/journal.pone.0251765>
- ALONSO-GONZÁLEZ M., FERNÁNDEZ-CARBALLIDO A., QUISPE-CHAUCAP, LOZZA I., MARTÍN-SABROSO C., ISABEL FRAGUAS-SÁNCHEZ A. (2022). DoE-based development of celecoxib loaded PLGA nanoparticles: In ovo assessment of its antiangiogenic effect. *European Journal of Pharmaceutics and Biopharmaceutics* 180: 149-160. <https://doi.org/10.1016/j.ejpb.2022.09.022>
- ALPHANDÉRY E. (2018). Glioblastoma Treatments: An Account of Recent Industrial Developments. *Frontiers in Pharmacology* 9: 879. <https://doi.org/10.3389/fphar.2018.00879>
- AMBASTA R. K., JHA S. K., KUMAR D., SHARMA R., JHA N. K., KUMAR P. (2015). Comparative study of anti-angiogenic activities of luteolin, lectin and lupeol biomolecules. *Journal of Translational Medicine* 13: 307. <https://doi.org/10.1186/s12967-015-0665-z>
- ANDACHT T., HU W., IVARIE R. (2004). Rapid and improved method for windowing eggs accessing the stage X chicken embryo. *Molecular Reproduction and Development* 69: 31-34. <https://doi.org/10.1002/mrd.20155>
- AUERBACH R., KUBAI L., KNIGHTON D., FOLKMAN J. (1974). A simple procedure for the long-term cultivation of chicken embryos. *Developmental Biology* 41: 391-394. [https://doi.org/10.1016/0012-1606\(74\)90316-9](https://doi.org/10.1016/0012-1606(74)90316-9)
- AUSPRUNK D. H., KNIGHTON D. R., FOLKMAN J. (1974). Differentiation of vascular endothelium in the chick chorioallantois: A structural and autoradiographic study. *Developmental Biology* 38: 237-248. [https://doi.org/10.1016/0012-1606\(74\)90004-9](https://doi.org/10.1016/0012-1606(74)90004-9)
- AVRAM S., CORICOVAC D. E., PAVEL I. Z., PINZARU I., GHIULAI R., BADERCA F., SOICA C., MUNTEAN D., BRANISTEANU D. E., SPANDIDOS D. A., TSATSAKIS A. M., DEHELEAN C. A. (2017). Standardization of A375 human melanoma models on chicken embryo chorioallantoic membrane and Balb/c nude mice. *Oncology Reports* 38: 89-99. <https://doi.org/10.3892/or.2017.5658>
- BABAE N., BOURAJAJ M., LIU Y., VAN BEIJNUM J. R., CERISOLI F., SCARIA P. V., VERHEUL M., VAN BERKEL M. P., PIETERS E. H. E., VAN HAASSTERT R. J., YOUSEFI A., MASTROBATTISTA E., STORM G., BEREZIKOV E., CUPPEN E., WOODLE M., SCHAAPVELD R. Q. J., PREVOST G. P., GRIFFIOEN A. W., VAN NOORT P. I., SCHIFFELERS R. M. (2014). Systemic miRNA-7 delivery inhibits tumor angiogenesis and growth in murine xenograft glioblastoma. *Oncotarget* 5: 6687-6700. <https://doi.org/10.18632/oncotarget.2235>
- BAHARARA J., NAMVAR F., MOUSAVI M., RAMEZANI T., MOHAMAD R. (2014). Anti-Angiogenesis Effect of Biogenic Silver Nanoparticles Synthesized Using Saliva officinalis on Chick Chorioallantoic Membrane (CAM). *Molecules* 19: 13498-13508. <https://doi.org/10.3390/molecules190913498>
- BALAKRISHNAN S., BHAT F. A., RAJA SINGH P., MUKHERJEE S., ELUMALAI P., DAS S., PATRA C. R., ARUNAKARAN J. (2016). Gold nanoparticle-conjugated quercetin inhibits epithelial-mesenchymal transition, angiogenesis and invasiveness via EGFR / VEGFR -2-mediated pathway in breast cancer. *Cell Proliferation* 49: 678-697. <https://doi.org/10.1111/cpr.12296>
- BOCCI G., FALCONE A., FIORAVANTI A., ORLANDI P., DI PAOLO A., FANELLI G., VIACAVA P., NACCARATO A. G., KERBEL R. S., DANESI R., DEL TACCA M., ALLEGRI G. (2008). Antiangiogenic and anticolorrectal cancer effects of metronomic irinotecan chemotherapy alone and in combination with semaxinib. *British Journal of Cancer* 98: 1619-1629. <https://doi.org/10.1038/sj.bjc.6604352>
- BORWOMPINYO S., BRAKE J., MOZDZIAK P. E., PETITTE J. N. (2005). Culture of chicken embryos in surrogate eggshells. *Poultry Science* 84: 1477-1482. <https://doi.org/10.1093/ps/84.9.1477>
- BOSTON UNIVERSITY (2023). *Animal care & use: Fertilized and Embryonated Chicken Eggs*. <https://www.bu.edu/research/ethics-compliance/animal-subjects/animal-care/fertilized-and-embryonated-chicken-eggs>.
- BROWN UNIVERSITY (2019). *Institutional Animal Care and Use Committee (IACUC). Policy for Use of Avian Embryos*. <https://www.brown.edu/research/sites/research/files/policies/Avian%20Embryo%20Use%20Policy%2011Jan19.pdf>
- BUSKOHL P. R., GOULD R. A., CURRAN S., ARCHER S. D., BUTCHER J. T. (2012). Multidisciplinary Inquiry-Based Investigation Learning Using an Ex Ovo Chicken Culture Platform: Role of Vitamin A on Embryonic Morphogenesis. *The American Biology Teacher* 74: 636-643. <https://doi.org/10.1525/abt.2012.74.9.7>
- CCSEA (2023). *Experiments Involving Samples from Slaughter House and Live Chick Embryo*. <https://ccsea.gov.in/WriteReadData/LnPdf/ExperimentsInvolvingSamplesfromSlaughterHouse.pdf>
- CHANDRAKALA V., ARUNA V., ANGAJALA G. (2022). Review on metal nanoparticles as nanocarriers: current challenges and perspectives in drug delivery systems. *Emergent Materials* 5: 1593-1615. <https://doi.org/10.1007/s42247-021-00335-x>
- CHAUHAN V. P., STYLIANOPOULOS T., MARTIN J. D., POPOVIĆ Z., CHENO., KAMOUN W. S., BAWENDI M. G., FUKUMURA D., JAIN R. K. (2012). Normalization of tumour blood vessels improves the delivery of nanomedicines in a size-dependent manner. *Nature Nanotechnology* 7: 383-388. <https://doi.org/10.1038/nnano.2012.45>
- CHEN D., LI D., XU X., QIU S., LUO S., QIU E., RONG Z., ZHANG J., ZHENG D. (2019). Galangin inhibits epithelial-mesenchymal transition and angiogenesis by downregulating CD44 in glioma. *Journal of Cancer* 10: 4499-4508. <https://doi.org/10.7150/jca.31487>
- CHEN J., CHEN A. Y., HUANG H., YE X., ROLLYSON W., PERRY H. E., BROWN K. C., ROJANASAKUL Y., RANKIN G. O., DASGUPTA P., CHEN Y. C. (2015). The flavonoid nobiletin inhibits tumor growth and angiogenesis of ovarian cancers via the Akt pathway. *International Journal of Oncology* 46: 2629-2638. <https://doi.org/10.3892/ijo.2015.2946>
- CHOI Y. S., JANG H., GUPTA B., JEONG J. H., GE Y., YONG C. S., KIM J. O., BAE J. S., SONG I. S., KIM I. S., LEE Y. M. (2020). Tie2-mediated vascular remodeling by ferritin-based protein C nanoparticles confers antitumor and anti-metastatic activities. *Journal of Hematology & Oncology* 13: 123. <https://doi.org/10.1186/s13045-020-00952-9>
- CHUANG Y. L., FANG H. W., AJITSARIA A., CHEN K. H., SU C. Y., LIU G. S., TSENG C. L. (2019). Development of Kaempferol-Loaded Gelatin Nanoparticles for the Treatment of Corneal Neovascularization in Mice. *Pharmaceutics* 11: 635. <https://doi.org/10.3390/pharmaceutics11120635>
- CONTE C., MORET F., ESPOSITO D., DAL POGGETTO G., AVITABILE C., UNGARO F., ROMANELLI A., LAURIENZO P., REDDI E., QUAGLIA F. (2019). Biodegradable nanoparticles exposing a short anti-FLT1 peptide as antiangiogenic platform to complement docetaxel anticancer activity. *Materials Science and Engineering: C* 102: 876-886. <https://doi.org/10.1016/j.msec.2019.04.054>
- CRESPINO P., CASAR B. (2016). The Chick Embryo Chorioallantoic Membrane as an in vivo Model to Study Metastasis. *Bio-protocol* 6: e1962. <https://doi.org/10.21769/BioProtoc.1962>
- DA COSTA P. M., DA COSTA M. P., CARVALHO A. A., CAVALCANTI S. M. T., DE OLIVEIRA CARDOSO M. V., DE OLIVEIRA FILHO G. B., DE ARAÚJO VIANA D., FECHINE-JAMACARU F. V., LEITE A. C. L., DE MORAES M. O., PESSOA C., FERREIRA P. M. P. (2015). Improvement of in vivo anticancer and antiangiogenic potential of thalidomide derivatives. *Chemico-Biological Interactions* 239: 174-183. <https://doi.org/10.1016/j.cbi.2015.06.037>
- DAI J., LIN Y., DUAN Y., LI Z., ZHOU D., CHEN W., WANG L., ZHANG Q. Q. (2017). Andrographolide Inhibits Angiogenesis by Inhibiting the Mir-21-5p/TIMP3 Signaling Pathway. *International Journal of Biological Sciences* 13: 660-668. <https://doi.org/10.7150/ijbs.19194>
- DERYUGINA E. I., QUIGLEY J. P. (2008). Chick embryo chorioallantoic membrane model systems to study and visualize human tumor cell metastasis. *Histochemistry and Cell Biology* 130: 1119-1130. <https://doi.org/10.1007/s00418-008-0536-2>
- DHARA M., ADHIKARI L., MAJUMDER R. (2018). Chorioallantoic Membrane (CAM) Assay of Different Extracts of Rhizome and Inflorescence of Heliconia rostrata. *Indian Journal of Pharmaceutical Education and Research* 52: S246-S251. <https://doi.org/10.5530/ijper.52.4s.104>
- DOHLE D. S., PASA S. D., GUSTMANN S., LAUB M., WISSLER J. H., JENNISSSEN H. P., DÜNKER N. (2009). Chick ex ovo culture and ex ovo CAM assay: how it really works. *Journal of visualized experiments: JoVE* (33): 1620. <https://doi.org/10.3791/1620>

- DORRELL M. I., MARCACCI M., BRAVO S., KURZ T., TREMBLAY J., RUSING J. C. (2012). Ex Ovo Model for Directly Visualizing Chick Embryo Development. *The American Biology Teacher* 74: 628-634. <https://doi.org/10.1525/abt.2012.74.9.6>
- DUGAN J. D., LAWTON M. T., GLASER B., BREM H. (1991). A new technique for explantation and in vitro cultivation of chicken embryos. *The Anatomical Record* 229: 125-128. <https://doi.org/10.1002/ar.1092290114>
- DUNN B. E., BOONE M. A. (1978). Photographic Study of Chick Embryo Development In vitro. *Poultry Science* 57: 370-377. <https://doi.org/10.3382/ps.0570370>
- DUNN B. E., FITZHARRIS T. P., BARNETT B. D. (1981). Effects of varying chamber construction and embryo pre-incubation age on survival and growth of chick embryos in shell-less culture. *The Anatomical Record* 199: 33-43. <https://doi.org/10.1002/ar.1091990105>
- DUPONT E., FALARDEAU P., MOUSA S. A., DIMITRIADOU V., PEPIN M. C., WANG T., ALAOUJ-JAMALI M. A. (2002). Antiangiogenic and antimetastatic properties of Neovastat (AE-941), an orally active extract derived from cartilage tissue. *Clinical and Experimental Metastasis* 19: 145-153. <https://doi.org/10.1023/A:1014546909573>
- DURUPT F., KOPPERS-LALIC D., BALME B., BUDEL L., TERRIERO, LINA B., THOMAS L., HOEBEN R. C., ROSA-CALATRAVA M. (2012). The chicken chorioallantoic membrane tumor assay as model for qualitative testing of oncolytic adenoviruses. *Cancer Gene Therapy* 19: 58-68. <https://doi.org/10.1038/cgt.2011.68>
- ECKRICH J., KUGLER P., BUHR C. R., ERNST B. P., MENDLER S., BAUMGART J., BRIEGER J., WIESMANN N. (2020). Monitoring of tumor growth and vascularization with repetitive ultrasonography in the chicken chorioallantoic-membrane assay. *Scientific Reports* 10: 18585. <https://doi.org/10.1038/s41598-020-75660-y>
- ESTERUELAS G., SOUTO E. B., ESPINAM, GARCÍA M. L., ŚWITALSKAM, WIETRZYK J., GLISZCZYŃSKA A., SÁNCHEZ-LÓPEZ E. (2022). Diclofenac Loaded Biodegradable Nanoparticles as Antitumoral and Antiangiogenic Therapy. *Pharmaceutics* 15: 102. <https://doi.org/10.3390/pharmaceutics15010102>
- EUROPEAN PARLIAMENT AND UNION (2010). *Directive 2010/63/EU of the European Parliament and of the Council of 22 September 2010 on the protection of animals used for scientific purposes Text with EEA relevance*. <http://data.europa.eu/eli/dir/2010/63/oj>
- FARCAS C. G., DEHELEAN C., PINZARU I. A., MIOC M., SOCOLIUC V., MOACA E. A., AVRAM S., GHIULAI R., CORICOVAD, PAVEL I., ALLA P. K., CRETU O. M., SOICA C., LOGHIN F. (2020). Theomoesensitive Betulinic Acid-Loaded Magnetoliposomes: A Promising Antitumor Potential for Highly Aggressive Human Breast Adenocarcinoma Cells Under Hyperthermic Conditions. *International Journal of Nanomedicine* Volume 15: 8175-8200. <https://doi.org/10.2147/IJN.S269630>
- FARZANEH M., ATTARI F., KHOSH NAM S. E., MOZDZIAK P. E. (2018). The method of chicken whole embryo culture using the eggshell windowing, surrogate eggshell and ex ovo culture system. *British Poultry Science* 59: 240-244. <https://doi.org/10.1080/00071668.2017.1413234>
- GAO Y., RANKIN G. O., TU Y., CHEN Y. C. (2016). Theaflavin-3, 3'-digallate decreases human ovarian carcinoma OVCAR-3 cell-induced angiogenesis via Akt and Notch-1 pathways, not via MAPK pathways. *International Journal of Oncology* 48: 281-292. <https://doi.org/10.3892/ijo.2015.3257>
- GARCÍA-PINEL B., PORRAS-ALCALÁ C., ORTEGA-RODRÍGUEZ A., SARABIA F., PRADOS J., MELGUIZO C., LÓPEZ-ROMERO J. M. (2019). Lipid-Based Nanoparticles: Application and Recent Advances in Cancer Treatment. *Nanomaterials* 9: 638. <https://doi.org/10.3390/nano9040638>
- GARRIER J., RESHETOV V., GRÄFE S., GUILLEMIN F., ZORIN V., BEZDETNYAYA L. (2014). Factors affecting the selectivity of nanoparticle-based photoinduced damage in free and xenografted chorioallantoic membrane model. *Journal of Drug Targeting* 22: 220-231. <https://doi.org/10.3109/1061186X.2013.860981>
- GOLDIE L. C., NIX M. K., HIRSCHI K. K. (2008). Embryonic vasculogenesis and hematopoietic specification. *Organogenesis* 4: 257-263. <https://doi.org/10.4161/org.4.4.7416>
- GUÉDES A. P. M., MELLO-ANDRADE F., PIRES W. C., DE SOUSA M. A. M., DA SILVA P. F. F., DE CAMARGO M. S., GEMEINER H., AMAURI M. A., GOMES CARDOSO C., DE MELO REIS P. R., SILVEIRA-LACERDA E. P., BATISTA A. A. (2020). Heterobimetallic Ru(II)/Fe(II) complexes as potent anticancer agents against breast cancer cells, inducing apoptosis through multiple targets. *Metallomics* 12: 547-561. <https://doi.org/10.1039/c9mt00272c>
- HARPER K., YATSYNA A., CHARBONNEAU M., BROCHU-GAUDREAU K., PERREAULT A., JELDRES C., MCDONALD P. P., DUBOIS C. M. (2021). The Chicken Chorioallantoic Membrane Tumor Assay as a Relevant In Vivo Model to Study the Impact of Hypoxia on Tumor Progression and Metastasis. *Cancers* 13: 1093. <https://doi.org/10.3390/cancers13051093>
- HOMAYOUNI-TABRIZI M., SOLTANI M., KARIMI E., NAMVAR F., POURESMAEIL V., ES-HAGHI A. (2019). Putative mechanism for anticancer properties of Ag-NPs (NPs) extract. *IET Nanobiotechnology* 13: 617-620. <https://doi.org/10.1049/iet-nbt.2018.5199>
- HOSHYAR N., GRAY S., HAN H., BAO G. (2016). The effect of nanoparticle size on in vivo pharmacokinetics and cellular interaction. *Nanomedicine* 11: 673-692. <https://doi.org/10.2217/nnm.16.5>
- HU J., ISHIHARA M., CHIN A. I., WU L. (2019). Establishment of xenografts of urological cancers on chicken chorioallantoic membrane (CAM) to study metastasis. *Precision Clinical Medicine* 2: 140-151. <https://doi.org/10.1093/pcmedi/pbz018>
- HUANG H., CHEN A. Y., ROJANASAKUL Y., YE X., RANKIN G. O., CHEN Y. C. (2015). Dietary compounds galangin and myricetin suppress ovarian cancer cell angiogenesis. *Journal of Functional Foods* 15: 464-475. <https://doi.org/10.1016/j.jff.2015.03.051>
- HUANG Y., ZHAO K., HU Y., ZHOU Y., LUO X., LI X., WEI L., LI Z., YOU Q., GUO Q., LU N. (2016). Wogonoside inhibits angiogenesis in breast cancer via suppressing Wnt/ β -catenin pathway. *Molecular Carcinogenesis* 55: 1598-1612. <https://doi.org/10.1002/mc.22412>
- HUBRECHT R. C., CARTER E. (2019). The 3Rs and Humane Experimental Technique: Implementing Change. *Animals* 9: 754. <https://doi.org/10.3390/ani9100754>
- ILLINOIS URBANA-CHAMPAIGN (2023). *Embryonated Avian Eggs in Research and Teaching*. <https://animalcare.illinois.edu/policies/embryonated-avian-eggs-research-and-teaching>
- INDRAKUMAR J., KORRAPATI P. S. (2020). Steering Efficacy of Nano Molybdenum Towards Cancer: Mechanism of Action. *Biological Trace Element Research* 194: 121-134. <https://doi.org/10.1007/s12011-019-01742-2>
- JAKOBSON M., HAHNENBERGER R., MAGNUSSON A. (1989). A Simple Method for Shell-less Cultivation of Chick Embryos. *Pharmacology & Toxicology* 64: 193-195. <https://doi.org/10.1111/j.1600-0773.1989.tb00629.x>
- JANSER F., NEY P., PINTO M., LANGER R., TSCHAN M. (2019). The Chick Chorioallantoic Membrane (CAM) Assay as a Three-dimensional Model to Study Autophagy in Cancer Cells. *BIO-PROTOCOL* 9: e3290. <https://doi.org/10.21769/BioProtoc.3290>
- JIANG W., KIM B. Y. S., RUTKA J. T., CHAN W. C. W. (2008). Nanoparticle-mediated cellular response is size-dependent. *Nature Nanotechnology* 3: 145-150. <https://doi.org/10.1038/nnano.2008.30>
- KAMIHIRA M., OGUCHI S., TACHIBANA A., KITAGAWA Y., IJIMA S. (1998). Improved hatching for in vitro quail embryo culture using surrogate eggshell and artificial vessel. *Development, Growth & Differentiation* 40: 449-455. <https://doi.org/10.1046/j.1440-169X.1998.t01-2-00010.x>
- KARAGIANNI F., PIPERI C., CASAR B., DE LA FUENTE-VIVAS D., GARCÍA-GÓMEZ R., LAMPADAKI K., PAPPAS V., PAPADAVI D. (2022). Combination of Resminostat with Ruxolitinib Exerts Antitumor Effects in the Chick Embryo Chorioallantoic Membrane Model for Cutaneous T Cell Lymphoma. *Cancers* 14: 1070. <https://doi.org/10.3390/cancers14041070>
- KAUSHIK S. (2021). *Handbook of Polymer and Ceramic Nanotechnology*. Springer, pp. 1293-1308. https://doi.org/10.1007/978-3-030-40513-7_39
- KAVALIAUSKAITĖ D., STAKIŠAITIS D., MARTINKUTĖ J., ŠLEKIENĖ L., KAZLAUSKAS A., BALNYTĖ I., LESAUŠKAITĖ V., VALANČIŪTĖ A. (2017). The Effect of Sodium Valproate on the Glioblastoma U87 Cell Line Tumor Development on the Chicken Embryo Chorioallantoic Membrane and on EZH2 and p53 Expression. *BioMed Research International* 2017: 1-12. <https://doi.org/10.1155/2017/6326053>
- KHAN I., SAEED K., KHAN I. (2019). Nanoparticles: Properties, applications and toxicities. *Arabian Journal of Chemistry* 12: 908-931. <https://doi.org/10.1016/j.arabjc.2017.05.011>
- KIM Y. J., HAN J. M., JUNG H. J. (2021). Antiangiogenic and antitumor potential of berbamine, a natural CaMKII γ inhibitor, against glioblastoma. *Biochemical and Biophysical Research Communications* 566: 129-134. <https://doi.org/10.1016/j.bbrc.2021.06.025>
- KLINGENBERG M., BECKER J., EBERTH S., KUBE D., WILTING J. (2014). The chick chorioallantoic membrane as an in vivo xenograft model for Burkitt lymphoma. *BMC Cancer* 14: 339. <https://doi.org/10.1186/1471-2407-14-339>
- KNIGHTON D. R., FIEGEL V. D., PHILLIPS G. D. (1991). The assay of angiogenesis. *Progress in clinical and biological research* 365: 291-299.
- KOHLI N., SAWADKAR P., HO S., SHARMA V., SNOW M., POWELL S., WOODRUFF M. A., HOOK L., GARCÍA-GARETA E. (2020). Pre-screening the intrinsic angiogenic capacity of biomaterials in an optimised ex ovo chorioallantoic membrane model. *Journal of Tissue Engineering* 11: 204173142090162. <https://doi.org/10.1177/2041731420901621>

- KUBIS N., LEVY B.I. (2003). Vasculogenesis and Angiogenesis: Molecular and Cellular Controls. *Interventional Neuroradiology* 9: 227-237. <https://doi.org/10.1177/159101990300900301>
- KUNZ P., SCHENKER A., SÄHR H., LEHNER B., FELLEBERG J. (2019). Optimization of the chicken chorioallantoic membrane assay as reliable in vivo model for the analysis of osteosarcoma. *PLOS ONE* 14: e0215312. <https://doi.org/10.1371/journal.pone.0215312>
- LEE H.P., LIU Y.C., CHEN P.C., TAI H.C., LI T.M., FONG Y.C., CHANG C.S., WU M.H., CHIU L.P., WANG C.J., CHEN Y.H., WU Y.J., TANG C.H., WANG S.W. (2017). Tanshinone IIA inhibits angiogenesis in human endothelial progenitor cells in vitro and in vivo. *Oncotarget* 8: 109217-109227. <https://doi.org/10.18632/oncotarget.22649>
- LEENE W., DUYZINGS M. J. M., STEEG C. (1973). Lymphoid stem cell identification in the developing thymus and bursa of fabricius of the chick. *Zeitschrift für Zellforschung und mikroskopische Anatomie* 136: 521-533. <https://doi.org/10.1007/BF00307368>
- LI B., JIANG Z., XIE D., WANG Y., LAO X. (2018). Cetuximab-modified CuS nanoparticles integrating near-infrared-II-responsive photothermal therapy and anti-vessel treatment. *International Journal of Nanomedicine* Volume 13: 7289-7302. <https://doi.org/10.2147/IJN.S175334>
- LI B., TONG T., REN N., RANKIN G. O., ROJANASAKUL Y., TU Y., CHEN Y. C. (2021). Theasaponin E1 Inhibits Platinum-Resistant Ovarian Cancer Cells through Activating Apoptosis and Suppressing Angiogenesis. *Molecules* 26: 1681. <https://doi.org/10.3390/molecules26061681>
- LI M., PATHAK R. R., LOPEZ-RIVERA E., FRIEDMAN S. L., AGUIRRE-GHISO J. A., SIKORA A. G. (2015). The In Ovo Chick Chorioallantoic Membrane (CAM) Assay as an Efficient Xenograft Model of Hepatocellular Carcinoma. *Journal of Visualized Experiments*: e52411. <https://doi.org/10.3791/52411>
- LI Q., WANG Y., ZHANG L., CHEN L., DU Y., YE T., SHI X. (2016). Naringenin exerts anti-angiogenic effects in human endothelial cells: Involvement of ERK/VEGF/KDR signaling pathway. *Fitoterapia* 111: 78-86. <https://doi.org/10.1016/j.fitote.2016.04.015>
- LI W., YALCIN M., BHARALI D. J., LIN Q., GODUGU K., FUJIOKA K., KEATING K. A., MOUSA S. A. (2019). RETRACTED ARTICLE: Pharmacokinetics, Biodistribution, and Anti-Angiogenesis Efficacy of Diamino Propane Tetraiodoacetic Acid-conjugated Biodegradable Polymeric Nanoparticle. *Scientific Reports* 9: 9006. <https://doi.org/10.1038/s41598-019-44979-6>
- LIAO Z.H., ZHU H.Q., CHEN Y.Y., CHEN R.L., FUL X., LIL., ZHOU H., ZHOU J.L., LIANG G. (2020). The epigallocatechin gallate derivative Y6 inhibits human hepatocellular carcinoma by inhibiting angiogenesis in MAPK/ERK1/2 and PI3K/AKT/ HIF-1 α /VEGF dependent pathways. *Journal of Ethnopharmacology* 259: 112852. <https://doi.org/10.1016/j.jep.2020.112852>
- LIU C., HE L., WANG J., WANG Q., SUN C., LI Y., JIA K., WANG J., XU T., MING R., WANG Q., LIN N. (2020). Anti-angiogenic effect of Shikonin in rheumatoid arthritis by downregulating PI3K/AKT and MAPKs signaling pathways. *Journal of Ethnopharmacology* 260: 113039. <https://doi.org/10.1016/j.jep.2020.113039>
- LIU J., ZHANG X., LI G., XU F., LI S., TENG L., LI Y., SUN F. (2019). Anti-Angiogenic Activity Of Bevacizumab-Bearing Dexamethasone-Loaded PLGA Nanoparticles For Potential Intravitreal Applications. *International journal of nanomedicine* 14: 8819-8834. <https://doi.org/10.2147/IJN.S217038>
- LIU P., ZHANG Q., MI J., WANG S., XU Q., ZHUANG D., CHEN W., LIU C., ZHANG L., GUO J., WU X. (2022). Exosomes derived from stem cells of human deciduous exfoliated teeth inhibit angiogenesis in vivo and in vitro via the transfer of miR-100-5p and miR-1246. *Stem Cell Research & Therapy* 13: 89. <https://doi.org/10.1186/s13287-022-02764-9>
- LOKMAN N. A., ELDER A. S. F., RICCIARDELLI C., OEHLER M. K. (2012). Chick Chorioallantoic Membrane (CAM) Assay as an In Vivo Model to Study the Effect of Newly Identified Molecules on Ovarian Cancer Invasion and Metastasis. *International Journal of Molecular Sciences* 13: 9959-9970. <https://doi.org/10.3390/ijms13089959>
- LU Y., WEN Q., LUO J., XIONG K., WU Z.X., WANG B.Q., CHEN Y., YANG B., FU S.Z. (2020). Self-assembled dihydroartemisinin nanoparticles as a platform for cervical cancer chemotherapy. *Drug Delivery* 27: 876-887. <https://doi.org/10.1080/10717544.2020.1775725>
- LUGANO R., RAMACHANDRAN M., DIMBERG A. (2020). Tumor angiogenesis: causes, consequences, challenges and opportunities. *Cellular and Molecular Life Sciences* 77: 1745-1770. <https://doi.org/10.1007/s00018-019-03351-7>
- MA J., LIU J., LUC W., CAID F. (2015a). Pachymic acid modified carbon nanoparticles reduced angiogenesis via inhibition of MMP-3. *International journal of clinical and experimental pathology* 8: 5464-5470.
- MA J., ZHANG Y., LI R., YE J., LI H., ZHANG Y., MA Z., LI J., ZHONG X., YANG X. (2015b). Tetrandrine suppresses human glioma growth by inhibiting cell survival, proliferation and tumour angiogenesis through attenuating STAT3 phosphorylation. *European Journal of Pharmacology* 764: 228-239. <https://doi.org/10.1016/j.ejphar.2015.06.017>
- MA Q., CHEN W., CHEN W. (2016). Anti-tumor angiogenesis effect of a new compound: B-9-3 through interference with VEGFR2 signaling. *Tumor Biology* 37: 6107-6116. <https://doi.org/10.1007/s13277-015-4473-0>
- MAHOR A., SINGH P. P., BHARADWAJ P., SHARMA N., YADAV S., ROSENHOLM J. M., BANSAL K. K. (2021). Carbon-Based Nanomaterials for Delivery of Biologicals and Therapeutics: A Cutting-Edge Technology. *C* 7: 19. <https://doi.org/10.3390/c7010019>
- MANGIR N., DIKICI S., CLAEYSSENS F., MACNEIL S. (2019). Using ex Ovo Chick Chorioallantoic Membrane (CAM) Assay To Evaluate the Biocompatibility and Angiogenic Response to Biomaterials. *ACS Biomaterials Science & Engineering* 5: 3190-3200. <https://doi.org/10.1021/acsbmaterials.9b00172>
- MANGIR N., RAZAA., HAYCOCK J.W., CHAPPLE C., MACNEIL S. (2018). An Improved In Vivo Methodology to Visualise Tumour Induced Changes in Vasculature Using the Chick Chorionic Allantoic Membrane Assay. *In Vivo* 32: 461-472. <https://doi.org/10.21873/invivo.11262>
- MANSUR A. A.P., PAIVA M. R.B., COTTA O. A.L., SILVA L. M., CARVALHO I. C., CAPANEMA N. S.V., CARVALHO S. M., COSTA A., MARTIN N. R., ECCO R., SANTOS B. S., FIALHO S. L., LOBATO Z. I.P., MANSUR H. S. (2022). Carboxymethylcellulose biofunctionalized ternary quantum dots for subcellular-targeted brain cancer nanotheranostics. *International Journal of Biological Macromolecules* 210: 530-544. <https://doi.org/10.1016/j.ijbiomac.2022.04.207>
- MARTOWICZ A., KERN J., GUNSILIUS E., UNTERGASSER G. (2015). Establishment of a Human Multiple Myeloma Xenograft Model in the Chicken to Study Tumor Growth, Invasion and Angiogenesis. *Journal of Visualized Experiments*: e52665. <https://doi.org/10.3791/52665-v>
- MELKONIAN G., MUNOZ N., CHUNG J., TONG C., MARR R., TALBOT P. (2002). Capillary plexus development in the day five to day six chick chorioallantoic membrane is inhibited by cytochalasin D and suramin. *Journal of Experimental Zoology* 292: 241-254. <https://doi.org/10.1002/jez.10014>
- MERLOS RODRIGO M. A., CASAR B., MICHALKOVA H., JIMENEZ JIMENEZ A. M., HEGER Z., ADAM V. (2021). Extending the Applicability of In Ovo and Ex Ovo Chicken Chorioallantoic Membrane Assays to Study Cytostatic Activity in Neuroblastoma Cells. *Frontiers in Oncology* 11: 707366. <https://doi.org/10.3389/fonc.2021.707366>
- MÎNDRILĂ I., BUTEICĂ S. A., MIHAIESCU D. E., BURADA F., MÎNDRILĂ B., PREDOI M. C., PIRICI I., FUDULU A., CROITORU O. (2017). Magnetic nanoparticles-based therapy for malignant mesothelioma. *Romanian journal of morphology and embryology = Revue roumaine de morphologie et embryologie* 58: 457-463.
- MITTAL A.K., BANERJEE U.C. (2016). Current status and future prospects of nanobiomaterials in drug delivery. In *Nanobiomaterials in Drug Delivery*. Applications of Nanobiomaterials, Vol. 9. Elsevier, pp. 147-170. <https://doi.org/10.1016/B978-0-323-42866-8.00005-8>
- MOHAMMAD G. R. K. S., TABRIZI M. H., ARDALAN T., YADAMANI S., SAFAVI E. (2019). Green synthesis of zinc oxide nanoparticles and evaluation of anti-angiogenesis, anti-inflammatory and cytotoxicity properties. *Journal of Biosciences* 44: 30. <https://doi.org/10.1007/s12038-019-9845-y>
- MOUSA S. A., O'CONNOR L., ROSSMAN T. G., BLOCK E. (2007). Pro-angiogenesis action of arsenic and its reversal by selenium-derived compounds. *Carcinogenesis* 28: 962-967. <https://doi.org/10.1093/carcin/bgl229>
- MOUSA S. A., YALCIN M., BHARALI D. J., MENG R., TANG H.Y., LIN H.Y., DAVIS F. B., DAVIS P. J. (2012). Tetraiodoacetic acid and its nanoformulation inhibit thyroid hormone stimulation of non-small cell lung cancer cells in vitro and its growth in xenografts. *Lung Cancer* 76: 39-45. <https://doi.org/10.1016/j.lungcan.2011.10.003>
- MURPHY J. B. (1914). Studies in tissue specificity. *Journal of Experimental Medicine* 19: 181-186. <https://doi.org/10.1084/jem.19.2.181>
- NAIK M., BRAHMA P., DIXIT M. (2018). A Cost-Effective and Efficient Chick Ex-Ovo CAM Assay Protocol to Assess Angiogenesis. *Methods and protocols* 1: 19. <https://doi.org/10.3390/mps1020019>
- NAIR R.M., REVU N.V. L., GALI S., KALLAMADI P.R., PRABHU V., MANUKONDA R., NEMANI H., KALIKI S., VEMUGANTI G.K. (2022). A short-term chick embryo in vivo xenograft model to study retinoblastoma cancer stem cells. *Indian Journal of Ophthalmology* 70: 1703. https://doi.org/10.4103/ijo.IJO_2348_21

- NKEMBO A. T., NTANTIE E., SALAKO O. O., AMISSAH F., POKU R. A., LATINWO L. M., LAMANGO N. S. (2016). The antiangiogenic effects of polyisoprenylated cysteinyl amide inhibitors in HUVEC, chick embryo and zebrafish is dependent on the polyisoprenyl moiety. *Oncotarget* 7: 68194-68205. <https://doi.org/10.18632/oncotarget.11908>
- NOWAK-SLIWINSKA P., BALLINI J.P., WAGNIÈRES G., VAN DEN BERGH H. (2010). Processing of fluorescence angiograms for the quantification of vascular effects induced by anti-angiogenic agents in the CAM model. *Microvascular Research* 79: 21-28. <https://doi.org/10.1016/j.mvr.2009.10.004>
- NOWAK-SLIWINSKA P., CLAVEL C. M., PĂUNESCU E., TE WINKEL M. T., GRIFFIOEN A. W., DYSON P. J. (2015). Antiangiogenic and Anticancer Properties of Bifunctional Ruthenium(II)-p-Cymene Complexes: Influence of Pendant Perfluorinated Chains. *Molecular Pharmaceutics* 12: 3089-3096. <https://doi.org/10.1021/acs.molpharmaceut.5b00417>
- PAL P., HALES K., PETRIK J., HALES D. B. (2019). Pro-apoptotic and anti-angiogenic actions of 2-methoxyestradiol and docosahexaenoic acid, the biologically derived active compounds from flaxseed diet, in preventing ovarian cancer. *Journal of Ovarian Research* 12: 49. <https://doi.org/10.1186/s13048-019-0523-3>
- PAN Y., LEIFERT A., RUAU D., NEUSS S., BORNEMANN J., SCHMID G., BRANDAU W., SIMON U., JAHNEN-DECHENT W. (2009). Gold Nanoparticles of Diameter 1.4 nm Trigger Necrosis by Oxidative Stress and Mitochondrial Damage. *Small* 5: 2067-2076. <https://doi.org/10.1002/sml.200900466>
- PASHA A., KUMBHAKAR D. V., SANA S. S., RAVINDER D., LAKSHMI B. V., KALANGI S. K., PAWAR S. C. (2022). Role of Biosynthesized Ag-NPs Using *Aspergillus niger* (MK503444.1) in Antimicrobial, Anti-Cancer and Anti-Angiogenic Activities. *Frontiers in Pharmacology* 12: 812474. <https://doi.org/10.3389/fphar.2021.812474>
- PATEL K. D., SINGH R. K., KIM H.W. (2019). Carbon-based nanomaterials as an emerging platform for theranostics. *Materials Horizons* 6: 434-469. <https://doi.org/10.1039/C8MH00966J>
- PEDROSA P., HEUER-JUNGEMANN A., KANARAS A. G., FERNANDES A. R., BAPTISTA P. V. (2017). Potentiating angiogenesis arrest in vivo via laser irradiation of peptide functionalised gold nanoparticles. *Journal of Nanobiotechnology* 15: 85. <https://doi.org/10.1186/s12951-017-0321-2>
- PINTO M. T., RIBEIRO A. S., CONDE I., CARVALHO R., PAREDES J. (2020). The Chick Chorioallantoic Membrane Model: A New In Vivo Tool to Evaluate Breast Cancer Stem Cell Activity. *International journal of molecular sciences* 22: 334. <https://doi.org/10.3390/ijms22010334>
- PION E., ASAM C., FEDER A.L., FELTHAUS O., HEIDEKRUEGER P. I., PRANTL L., HAERTEIS S., AUNG T. (2021). Laser speckle contrast analysis (LASCA) technology for the semiquantitative measurement of angiogenesis in in-ovo-tumor-model. *Microvascular Research* 133: 104072. <https://doi.org/10.1016/j.mvr.2020.104072>
- PIZON M., SCHOTT D., PACHMANN U., SCHOBERT R., PIZON M., WOZNIAK M., BOBINSKI R., PACHMANN K. (2022). Chick Chorioallantoic Membrane (CAM) Assays as a Model of Patient-Derived Xenografts from Circulating Cancer Stem Cells (cCSCs) in Breast Cancer Patients. *Cancers* 14: 1476. <https://doi.org/10.3390/cancers14061476>
- PONNUSAMY C., SUGUMARAN A., KRISHNASWAMI V., KANDASAMY R., NATESAN S. (2019). Design and development of artemisinin and dexamethasone loaded topical nanodispersion for the effective treatment of age-related macular degeneration. *IET Nanobiotechnology* 13: 868-874. <https://doi.org/10.1049/iet-nbt.2019.0130>
- POWER E. A., FERNANDEZ-TORRES J., ZHANG L., YAUN R., LUCIEN F., DANIELS D. J. (2022). Chorioallantoic membrane (CAM) assay to study treatment effects in diffuse intrinsic pontine glioma. *PLOS ONE* 17: e0263822. <https://doi.org/10.1371/journal.pone.0263822>
- REN H., ZHU C., LI Z., YANG W., SONG E. (2014). Emodin-Loaded Magnesium Silicate Hollow Nanocarriers for Anti-Angiogenesis Treatment through Inhibiting VEGF. *International Journal of Molecular Sciences* 15: 16936-16948. <https://doi.org/10.3390/ijms150916936>
- RIBATTI D. (2016). The chick embryo chorioallantoic membrane (CAM). A multifaceted experimental model. *Mechanisms of Development* 141: 70-77. <https://doi.org/10.1016/j.mod.2016.05.003>
- RIBATTI D., GUALANDRIS A., BASTAKI M., VACCA A., IUHLARO M., RONCALI L., PRESTA M. (1997). New Model for the Study of Angiogenesis and Antiangiogenesis in the Chick Embryo Chorioallantoic Membrane: The Gelatin Sponge/Chorioallantoic Membrane Assay. *Journal of Vascular Research* 34: 455-463. <https://doi.org/10.1159/000159256>
- RIDDERBUSCH I., BERGHOLZ R., FATTOUH M., ESCHENBURG G., ROTH B., APPL B., MAENNER J., REINSHAGEN K., KLUTH D. (2015). A Chicken Embryo Model for the Study of Umbilical and Supraumbilical Body Wall Malformations. *European Journal of Pediatric Surgery* 25: 257-261. <https://doi.org/10.1055/s-0034-1371718>
- ROBL J., PRATHER R., BARNES F., EYESTONE W., NORTHEY D., GILLIGAN B. (1991). The Public Health Service Responds to Commonly Asked Questions. *ILAR Journal* 33: 68-70. <https://doi.org/10.1093/ilar.33.4.68>
- ROMA-RODRIGUES C., HEUER-JUNGEMANN A., FERNANDES A. R., KANARAS A. G., BAPTISTA P. V. (2016). Peptide-coated gold nanoparticles for modulation of angiogenesis in vivo. *International journal of nanomedicine* 11: 2633-2639. <https://doi.org/10.2147/IJN.S108661>
- SADALAGE P. S., PATIL R. V., HAVALDARD V., GAVADE S. S., SANTOSA C., PAWAR K. D. (2021). Optimally biosynthesized, PEGylated gold nanoparticles functionalized with quercetin and camptothecin enhance potential anti-inflammatory, anti-cancer and anti-angiogenic activities. *Journal of Nanobiotechnology* 19: 84. <https://doi.org/10.1186/s12951-021-00836-1>
- SALEEM M., ASIF M., PARVEEN A., YASEEN H. S., SAADULLAH M., BASHIR A., ASIF J., ARIF M., KHAN I. U., KHAN R. U. (2021). Investigation of in vivo anti-inflammatory and anti-angiogenic attributes of coumarin-rich ethanolic extract of *Melilotus indicus*. *Inflammopharmacology* 29: 281-293. <https://doi.org/10.1007/s10787-020-00703-9>
- SAMAD N. A., ABDUL A. B., RAHMAN H. S., RASEDEE A., TENGKU IBRAHIM T. A., KEON Y. S. (2018). Zerumbone Suppresses Angiogenesis in HepG2 Cells through Inhibition of Matrix Metalloproteinase-9, Vascular Endothelial Growth Factor, and Vascular Endothelial Growth Factor Receptor Expressions. *Pharmacognosy magazine* 13: S731-S736. <https://doi.org/10.4103/pm.pm.18.17>
- SCHMITD L. B., LIU M., SCANLON C. S., BANERJEE R., D'SILVA N. J. (2019). The Chick Chorioallantoic Membrane In Vivo Model to Assess Perineural Invasion in Head and Neck Cancer. *Journal of Visualized Experiments*: e59296. <https://doi.org/10.3791/59296>
- SCOTT P.S., VRBA L.K., WILKS J.W. (1993). A Simple Vessel for the Culture of Chicken Embryos Used in Angiogenesis Assays. *Microvascular Research* 45: 324-327. <https://doi.org/10.1006/mvre.1993.1029>
- SHAH B. B., BAKSI R., CHAUDAGAR K. K., NIVSARKAR M., MEHTA A. A. (2018). Anti-leukemic and anti-angiogenic effects of d-Limonene on K562-implanted C57 BL/6 mice and the chick chorioallantoic membrane model. *Animal Models and Experimental Medicine* 1: 328-333. <https://doi.org/10.1002/ame2.12039>
- SHAH M., CABRERA-GHAYOURI S., CHRISTIE L. A., HELD K. S., VISWANATH V. (2019). Translational Preclinical Pharmacologic Disease Models for Ophthalmic Drug Development. *Pharmaceutical research* 36: 58. <https://doi.org/10.1007/s11095-019-2588-5>
- SHEIBANI N., WANG S., DARJATMOKO S. R., FISK D. L., SHAHI P. K., PATNAIK B. R., SORENSON C. M., BHOWMICK R., VOLPERT O. V., ALBERT D. M., MELGAR-ASENSIO I., HENKIN J. (2019). Novel anti-angiogenic PEDF-derived small peptides mitigate choroidal neovascularization. *Experimental Eye Research* 188: 107798. <https://doi.org/10.1016/j.exer.2019.107798>
- SHMUELI R. B., OHNAKA M., MIKI A., PANDEY N. B., LIMA E SILVA R., KOSKIMAKI J. E., KIM J., POPEL A. S., CAMPOCHIARO P. A., GREEN J. J. (2013). Long-term suppression of ocular neovascularization by intraocular injection of biodegradable polymeric particles containing a serpin-derived peptide. *Biomaterials* 34: 7544-7551. <https://doi.org/10.1016/j.biomaterials.2013.06.044>
- SHOIN K., YAMASHITA J., ENKAKU F., SASAKI T., TANAKA M., YOSHIO Y. (1991). Chick Embryo Assay as Chemosensitivity Test for Malignant Glioma. *Japanese Journal of Cancer Research* 82: 1165-1170. <https://doi.org/10.1111/j.1349-7006.1991.tb01772.x>
- SILVA L. S., VÉRAS J. H., FERNANDES A. S., DE MELO BISNETO A. V., DE CASTRO M. R. C., NAVES R. F., CARNEIRO C. C., PÉREZ C. N., CARDOSO C. G., RIBEIRO E SILVA C., CHEN-CHEN L. (2022). Novel sulfonamide-chalcone hybrid stimulates inflammation, angiogenesis and upregulates vascular endothelial growth factor (VEGF) in vivo. *Microvascular Research* 139: 104253. <https://doi.org/10.1016/j.mvr.2021.104253>
- SMITH J. D., FISHER G. W., WAGGONER A. S., CAMPBELL P. G. (2007). The use of quantum dots for analysis of chick CAM vasculature. *Microvascular Research* 73: 75-83. <https://doi.org/10.1016/j.mvr.2006.09.003>
- SON S., KIM N., YOU D. G., YOON H. Y., YHEE J. Y., KIM K., KWON I. C., KIM S. H. (2017). Antitumor therapeutic application of self-assembled RNAi-AuNP nanoconstructs: Combination of VEGF-RNAi and photothermal ablation. *Theranostics* 7: 9-22. <https://doi.org/10.7150/thno.16042>
- SUI H., ZHAO J., ZHOU L., WEN H., DENG W., LI C., JI Q., LIU X., FENG Y., CHAI N., ZHANG Q., CAI J., LI Q. (2017). Tanshinone IIA inhibits β -catenin/VEGF-mediated angiogenesis by targeting TGF- β 1 in normoxic and HIF-1 α in hypoxic microenvironments in human colorectal cancer. *Cancer Letters* 403: 86-97. <https://doi.org/10.1016/j.canlet.2017.05.013>

- SUN J., NIE H., PAN P., JIANG Q., LIU C., WANG M., DENG Y., YAN B. (2023). Combined Anti-Angiogenic and Anti-Inflammatory Nanof ormulation for Effective Treatment of Ocular Vascular Diseases. *International Journal of Nanomedicine* 18: 437-453. <https://doi.org/10.2147/IJN.S387428>
- SWADI R., MATHER G., PIZER B. L., LOSTY P. D., SEE V., MOSS D. (2018). Optimising the chick chorioallantoic membrane xenograft model of neuroblastoma for drug delivery. *BMC Cancer* 18: 28. <https://doi.org/10.1186/s12885-017-3978-x>
- SYSG., VAN BOCKSTAL M., FORSYTHR., BALKEM., POFFYN B., UYTENDAELE D., BRACKE M., DE WEVER O. (2012). Tumor grafts derived from sarcoma patients retain tumor morphology, viability, and invasion potential and indicate disease outcomes in the chick chorioallantoic membrane model. *Cancer Letters* 326: 69-78. <https://doi.org/10.1016/j.canlet.2012.07.023>
- SYSG. M.L., LAPEIRE L., STEVENS N., FAVOREEL H., FORSYTH R., BRACKE M., DE WEVER O. (2013). The In ovo CAM-assay as a Xenograft Model for Sarcoma. *Journal of Visualized Experiments*: e50522. <https://doi.org/10.3791/50522>
- TAHARA Y., OBARA K. (2014). A Novel Shell-less Culture System for Chick Embryos Using a Plastic Film as Culture Vessels. *The Journal of Poultry Science* 51: 307-312. <https://doi.org/10.2141/jpsa.0130043>
- TAHARA Y., OBARA K., KAMIHIRA M. (2021). Calcium carbonate supplementation to chorioallantoic membranes improves hatchability in shell-less chick embryo culture. *Journal of Bioscience and Bioengineering* 131: 314-319. <https://doi.org/10.1016/j.jbiosc.2020.11.001>
- TANNENBAUM J., BENNETT B. T. (2015). Russell and Burch's 3Rs then and now: the need for clarity in definition and purpose. *Journal of the American Association for Laboratory Animal Science*: JAALAS 54: 120-132.
- TOMAYKO M. M., REYNOLDS C. P. (1989). Determination of subcutaneous tumor size in athymic (nude) mice. *Cancer Chemotherapy and Pharmacology* 24: 148-154. <https://doi.org/10.1007/BF00300234>
- TUFAN A., SATIROGLU-TUFAN N. (2005). The Chick Embryo Chorioallantoic Membrane as a Model System for the Study of Tumor Angiogenesis, Invasion and Development of Anti-Angiogenic Agents. *Current Cancer Drug Targets* 5: 249-266. <https://doi.org/10.2174/15680090504064624>
- ULUS G., KOPARAL A. T., BAYSAL K., YETIK ANACAK G., KARABAY YAVAŞOĞLU N. (2018). The anti-angiogenic potential of (\pm) gossypol in comparison to suramin. *Cytotechnology* 70: 1537-1550. <https://doi.org/10.1007/s10616-018-0247-z>
- UVEZ A., AYDINLIK S., ESENER O. B. B., ERKISA M., KARAKUS D., ARMUTAK E. I. (2020). Synergistic interactions between resveratrol and doxorubicin inhibit angiogenesis both in vitro and in vivo. *Polish Journal of Veterinary Sciences* 23: 571-580. <https://doi.org/https://doi.org/10.24425/pjvs.2020.135803>
- VARGESSON N. (2003). Vascularization of the developing chick limb bud: role of the TGF β signalling pathway. *Journal of Anatomy* 202: 93-103. <https://doi.org/10.1046/j.1469-7580.2003.00133.x>
- VU B. T., SHAHIN S. A., CROISSANT J., FATIEIEV Y., MATSUMOTO K., LE-HOANG DOAN T., YIK T., SIMARGI S., CONTERAS A., RATLIFF L., JIMENEZ C. M., RAEHM L., KHASHAB N., DURAND J.O., GLACKIN C., TAMANOI F. (2018). Chick chorioallantoic membrane assay as an in vivo model to study the effect of nanoparticle-based anticancer drugs in ovarian cancer. *Scientific Reports* 8: 8524. <https://doi.org/10.1038/s41598-018-25573-8>
- WALKEY C., SYKES E. A., CHAN W. C. W. (2009). Application of semiconductor and metal nanostructures in biology and medicine. *Hematology* 2009: 701-707. <https://doi.org/10.1182/asheducation-2009.1.701>
- WANG J.H., TSENG C.L., LIN F.L., CHEN J., HSIEH E.H., LAMA S., CHUANG Y.F., KUMAR S., ZHU L., MCGUINNESS M. B., HERNANDEZ J., TU L., WANG P.Y., LIU G.S. (2022a). Topical application of TAK1 inhibitor encapsulated by gelatin particle alleviates corneal neovascularization. *Theranostics* 12: 657-674. <https://doi.org/10.7150/thno.65098>
- WANG T., LIU J., XIAO X.Q. (2015a). Cantharidin inhibits angiogenesis by suppressing VEGF-induced JAK1/STAT3, ERK and AKT signaling pathways. *Archives of Pharmacological Research* 38: 282-289. <https://doi.org/10.1007/s12272-014-0383-8>
- WANG Y., LI J.X., WANG Y.Q., MIAO Z.H. (2015b). Tanshinone I inhibits tumor angiogenesis by reducing STAT3 phosphorylation at TYR705 and hypoxia-induced HIF-1 α accumulation in both endothelial and tumor cells. *Oncotarget* 6: 16031-16042. <https://doi.org/10.18632/oncotarget.3648>
- WANG Z., SUN C., WU H., XIE J., ZHANG T., LI Y., XU X., WANG P., WANG C. (2022b). Cascade targeting codelivery of ingenol-3-angelate and doxorubicin for enhancing cancer chemoimmunotherapy through synergistic effects in prostate cancer. *Materials Today Bio* 13: 100189. <https://doi.org/10.1016/j.mtbio.2021.100189>
- XING L., SUN F., WANG Z., LI Y., YANG Z., WANG F., ZHAI G., TAN H. (2019). Characterization and bioactivity of self-assembled anti-angiogenic chondroitin sulfate-ES2-AF nanoparticle conjugate. *International Journal of Nanomedicine* 14: 2573-2589. <https://doi.org/10.2147/IJN.S195934>
- XU J., SONG M., FANG Z., ZHENG L., HUANG X., LIU K. (2023). Applications and challenges of ultra-small particle size nanoparticles in tumor therapy. *Journal of Controlled Release* 353: 699-712. <https://doi.org/10.1016/j.jconrel.2022.12.028>
- YALCIN H. C., SHEKHAR A., RANE A. A., BUTCHER J. T. (2010a). An ex-ovo Chicken Embryo Culture System Suitable for Imaging and Microsurgery Applications. *Journal of Visualized Experiments*: e2154. <https://doi.org/10.3791/2154>
- YALCIN M., BHARALI D. J., DYSKIN E., DIER E., LANSING L., MOUSA S. S., DAVIS F. B., DAVIS P. J., MOUSA S. A. (2010b). Tetraiodothyroacetic Acid and Tetraiodothyroacetic Acid Nanoparticle Effectively Inhibit the Growth of Human Follicular Thyroid Cell Carcinoma. *Thyroid* 20: 281-286. <https://doi.org/10.1089/thy.2009.0249>
- YALCIN M., BHARALI D. J., LANSING L., DYSKIN E., MOUSA S. S., HERCBERGS A., DAVIS F. B., DAVIS P. J., MOUSA S. A. (2009). Tetraiodothyroacetic acid (tetrac) and tetrac nanoparticles inhibit growth of human renal cell carcinoma xenografts. *Anticancer research* 29: 3825-3831.
- YALCIN M., DYSKIN E., LANSING L., BHARALI D. J., MOUSA S. S., BRIDOUX A., HERCBERGS A. H., LIN H. Y., DAVIS F. B., GLINSKY G. V., GLINSKII A., MA J., DAVIS P. J., MOUSA S. A. (2010c). Tetraiodothyroacetic Acid (Tetrac) and Nanoparticulate Tetrac Arrest Growth of Medullary Carcinoma of the Thyroid. *The Journal of Clinical Endocrinology & Metabolism* 95: 1972-1980. <https://doi.org/10.1210/jc.2009-1926>
- YAQOOB A. A., AHMAD H., PARVEEN T., AHMAD A., OVES M., ISMAIL I. M. I., QARI H. A., UMAR K., MOHAMAD IBRAHIM M. N. (2020). Recent Advances in Metal Decorated Nanomaterials and Their Various Biological Applications: A Review. *Frontiers in Chemistry* 8: 341. <https://doi.org/10.3389/fchem.2020.00341>
- YU M., HUANG S., YU K. J., CLYNE A. M. (2012). Dextran and Polymer Polyethylene Glycol (PEG) Coating Reduce Both 5 and 30 nm Iron Oxide Nanoparticle Cytotoxicity in 2D and 3D Cell Culture. *International Journal of Molecular Sciences* 13: 5554-5570. <https://doi.org/10.3390/ijms13055554>
- ZENG L., MA W., SHI L., CHEN X., WU R., ZHANG Y., CHEN H., CHEN H. (2019). Poly(lactic-co-glycolic acid) nanoparticle-mediated interleukin-12 delivery for the treatment of diabetic retinopathy. *International Journal of Nanomedicine* Volume 14: 6357-6369. <https://doi.org/10.2147/IJN.S214727>
- ZHANG J., ZHU J., ZHAO L., MAO K., GU Q., LI D., ZHAO J., WU X. (2021). RGD-modified multifunctional nanoparticles encapsulating salvianolic acid A for targeted treatment of choroidal neovascularization. *Journal of Nanobiotechnology* 19: 196. <https://doi.org/10.1186/s12951-021-00939-9>
- ZHANG X., BOHNER A., BHUVANAGIRI S., UEHARA H., UPADHYAY A. K., EMERSON L. L., BONDALAPATI S., MUDDANA S. K., FANG D., LI M., SANDHU Z., HUSSAIN A., CARROLL L. S., TIEM M., ARCHER B., KOMPPELLA U., PATIL R., AMBATI B. K. (2017). Targeted Intracellular Nanoparticle for Neovascular Macular Degeneration: Preclinical Dose Optimization and Toxicology Assessment. *Molecular therapy* 25: 1606-1615. <https://doi.org/10.1016/j.yymthe.2017.01.014>
- ZHAO Y., ADJEI A. A. (2015). Targeting Angiogenesis in Cancer Therapy: Moving Beyond Vascular Endothelial Growth Factor. *The oncologist* 20: 660-673. <https://doi.org/10.1634/theoncologist.2014-0465>
- ZHENG W., YANG L., LIU Y., QIN X., ZHOU Y., ZHOU Y., LIU J. (2014). Mo polyoxometalate nanoparticles inhibit tumor growth and vascular endothelial growth factor induced angiogenesis. *Science and Technology of Advanced Materials* 15: 035010. <https://doi.org/10.1088/1468-6996/15/3/035010>
- ZHOU Z., MAO W., LI Y., QI C., HE Y. (2019). Myricetin Inhibits Breast Tumor Growth and Angiogenesis by Regulating VEGF/VEGFR2 and p38MAPK Signaling Pathways. *The Anatomical Record* 302: 2186-2192. <https://doi.org/10.1002/ar.24222>
- ZHU P. T., MAO M., LIU Z. G., TAO L., YAN B. C. (2017). Scutellarin suppresses human colorectal cancer metastasis and angiogenesis by targeting ephrin2. *American journal of translational research* 9: 5094-5104.
- ZIYAD S., IRUELA-ARISPE M. L. (2011). Molecular Mechanisms of Tumor Angiogenesis. *Genes & Cancer* 2: 1085-1096. <https://doi.org/10.1177/1947601911432334>
- ZOU L., LIU X., LI J., LI W., ZHANG L., FU C., ZHANG J., GU Z. (2021). Redox-sensitive carrier-free nanoparticles self-assembled by disulfide-linked paclitaxel-tetramethylpyrazine conjugate for combination cancer chemotherapy. *Theranostics* 11: 4171-4186. <https://doi.org/10.7150/thno.42260>
- ZUO Z., SYROVETS T., WU Y., HAFNER S., VERNIKOUSKAYA I., LIU W., MA G., WEIL T., SIMMET T., RASCHE V. (2017). The CAM cancer xenograft as a model for initial evaluation of MR labelled compounds. *Scientific Reports* 7: 46690. <https://doi.org/10.1038/srep46690>